

to the upper cell surface was very inefficient even with coexpression of NA (upper PM only, 9%; PMs plus cytoplasmic compartments, 91% in HA and NA double-positive cells) (Fig. 3C) although the mechanisms that link the cell density to the apical transport kinetics of cargo proteins remain to be elucidated in future studies.

It has been suggested that the influenza virus utilizes lipid rafts in the apical PM as the sites of virus particle assembly and budding (5, 52). Immunoelectron microscopy has shown that HA is accumulated and clustered in lipid rafts on the cell surface, which provides a sufficient concentration of HA to mediate efficient virus replication (5). Consistent with this finding, our PLA analysis revealed that HA and NA likely accumulated at the TGN before they reached the apical PM (Fig. 10B). This analysis further revealed that the coexpression of HA and NA induced efficient clustering of lipid raft microdomains in the cytoplasmic compartments (Fig. 12). Selective incorporation of certain lipid components (cholesterol and sphingomyelin) into influenza virus particles has been suggested in a previous study based on detergent solubility in viral particle envelopes (52). It is conceivable that the lipid raft clustering induced by coexpression of HA and NA led to an increase in the curvature of the membrane, facilitating the generation of apical sorting/transport vesicles from the TGN, and finally to arrival at the budding site together.

Possible mechanisms of lipid raft clustering by coexpression of HA and NA. Recent studies have suggested that hydrophobic mismatch, i.e., the difference between the hydrophobic length of the TM proteins and the hydrophobic thickness of the membrane they span, is involved in lipid raft clustering (45). The sphingolipids, such as sphingomyelin, that constitute lipid rafts have saturated fatty acids longer than the unsaturated fatty acids of phospholipids, making the lipid rafts thicker than other membrane domains. In this model, it has been proposed that to avoid unfavorable exposure of the hydrophobic surfaces to hydrophilic environments, the TM proteins are incorporated into lipid microdomains, the hydrophobic thickness of which is equal to the hydrophobic length of the TM proteins (10, 45). The length of the TMD has also been suggested to regulate protein targeting to the PM in *Saccharomyces cerevisiae* (53, 54). The lengths of the TMDs of PR8 HA and NA are 27 and 29 amino acids, respectively, and are relatively long, considering that TMD helices are usually around 20 amino acids in length. It is conceivable that such longer TMDs in HA and NA contributed to lipid raft clustering, possibly by recruiting and stabilizing sphingolipids containing a bulky head group in the outer leaflet of the lipid bilayer.

A previous *in vitro* study using two TM peptides, one matching the thickness of raft lipids and the other the thickness of nonraft lipids (23 and 29 amino acids in length), showed that both peptides were primarily localized in nonraft microdomains (55). However, a recent study revealed that cholesterol constrains membranes containing TM peptides, thereby rearranging both lipid acyl chains and TM peptides according to hydrophobic length (56); this suggests that not only hydrophobic mismatch but also cholesterol is involved in the sorting and clustering of TM proteins in the lipid bilayer. We think that this possibility is likely in the case of the influenza virus since previous studies (4, 16) and our study repeatedly found that depletion of cholesterol resulted in a failure of lipid raft association and apical transport of HA.

Cholesterol and sphingolipids are critical components of lipid rafts. Cholesterol is comprised of three structurally distinct re-

gions: a hydroxyl group, a rigid steroid ring, and a flexible alkyl chain. The structure of cholesterol is characterized by a flat and smooth α -face containing only axial hydrogen atoms and a rough β -face containing bulky methyl groups. Lipids, including sphingolipids, generally interact with the α -face of cholesterol, leaving the β -face available for the TMD (57). Cholesterol can also form homodimers through the interaction with their respective smooth α -faces, leaving their opposite β -faces available for protein binding. For example, a cholesterol dimer can recruit two molecules of G protein-coupled receptor, thereby inducing receptor dimerization (58). In this study, we found that HA and NA were accumulated at the cytoplasmic compartments, most likely at the TGN, via their association with lipid rafts, and this accumulation was cholesterol dependent (Fig. 8 and 10).

Several previous studies on the influenza virus used the A/Udorn/72 (H3) strain and indicated that deletions or mutations in the TMD-CT of HA and NA impaired their lipid raft association without affecting apical targeting (5, 7). A kinetic analysis of the apical transport of the HA mutants showed only a 1-h delay to the cell surface compared with wt-HA (59). In contrast, we used the PR8 (H1) strain and showed that our similar nonraft HA mutants exhibited a great delay of transport to the apical PM (Fig. 9A). Another study used the A/Japan/305 (H2) strain and also showed a significant delay of its nonraft HA mutant to the cell surface (2). When we compared the amino acid sequences of the HA TMD-CTs, we found that the PR8 (H1) and A/Japan/305 (H2) shared 75.7% homology, the PR8 (H1) and A/Udorn/72 (H3) shared 37.8% homology, and the A/Japan/305 (H2) and A/Udorn/72 (H3) shared 32.4% homology. Thus, the structure and length of the TMD helices may differ widely among these three HAs. It is possible that the A/Udorn/72 HA may be transported to the cell surface in a less cholesterol-dependent manner.

ACKNOWLEDGMENTS

We thank Yoshihiro Kawaoka (University of Wisconsin—Madison, USA, and University of Tokyo, Japan) for providing us with Poll plasmids (pHH21) used for a reverse genetics system of influenza A virus, Ken Watanabe (Nagasaki University, Japan) for providing us with rabbit anti-M1 polyclonal antibody, and Naoki Takizawa (Institute of Microbial Chemistry, Japan) for MDCK-HA cells. We also thank Hiyori Haraguchi for technical assistance.

This work was supported by a Human Science grant from the Ministry of Health, Labor, and Welfare of Japan and by a Grant-in-Aid for Scientific Research from the Japan Society for the Promotion of Science.

REFERENCES

1. Nayak DP, Balogun RA, Yamada H, Zhou ZH, Barman S. 2009. Influenza virus morphogenesis and budding. *Virus Res.* 143:147–161. <http://dx.doi.org/10.1016/j.virusres.2009.05.010>.
2. Lin S, Naim HY, Rodriguez AC, Roth MG. 1998. Mutations in the middle of the transmembrane domain reverse the polarity of transport of the influenza virus hemagglutinin in MDCK epithelial cells. *J. Cell Biol.* 142:51–57. <http://dx.doi.org/10.1083/jcb.142.1.51>.
3. Barman S, Nayak DP. 2000. Analysis of the transmembrane domain of influenza virus neuraminidase, a type II transmembrane glycoprotein, for apical sorting and raft association. *J. Virol.* 74:6538–6545. <http://dx.doi.org/10.1128/JVI.74.14.6538-6545.2000>.
4. Scheiffele P, Roth MG, Simons K. 1997. Interaction of influenza virus haemagglutinin with sphingolipid-cholesterol membrane domains via its transmembrane domain. *EMBO J.* 16:5501–5508. <http://dx.doi.org/10.1093/emboj/16.18.5501>.
5. Takeda M, Leser GP, Russell CJ, Lamb RA. 2003. Influenza virus hemagglutinin concentrates in lipid raft microdomains for efficient viral fu-

- sion. *Proc. Natl. Acad. Sci. U. S. A.* 100:14610–14617. <http://dx.doi.org/10.1073/pnas.2235620100>.
6. Leser GP, Lamb RA. 2005. Influenza virus assembly and budding in raft-derived microdomains: a quantitative analysis of the surface distribution of HA, NA and M2 proteins. *Virology* 342:215–227. <http://dx.doi.org/10.1016/j.virol.2005.09.049>.
 7. Zhang J, Pekosz A, Lamb RA. 2000. Influenza virus assembly and lipid raft microdomains: a role for the cytoplasmic tails of the spike glycoproteins. *J. Virol.* 74:4634–4644. <http://dx.doi.org/10.1128/JVI.74.10.4634-4644.2000>.
 8. Chen BJ, Takeda M, Lamb RA. 2005. Influenza virus hemagglutinin (H3 subtype) requires palmitoylation of its cytoplasmic tail for assembly: M1 proteins of two subtypes differ in their ability to support assembly. *J. Virol.* 79:13673–13684. <http://dx.doi.org/10.1128/JVI.79.21.13673-13684.2005>.
 9. Rossman JS, Jing X, Leser GP, Lamb RA. 2010. Influenza virus M2 protein mediates ESCRT-independent membrane scission. *Cell* 142:902–913. <http://dx.doi.org/10.1016/j.cell.2010.08.029>.
 10. Magal LG, Yaffe Y, Shepshelovich J, Aranda JF, de Marco Mdel C, Gaus K, Alonso MA, Hirschberg K. 2009. Clustering and lateral concentration of raft lipids by the MAL protein. *Mol. Biol. Cell* 20:3751–3762. <http://dx.doi.org/10.1091/mbc.E09-02-0142>.
 11. Rodriguez-Boulan E, Kreitzer G, Musch A. 2005. Organization of vesicular trafficking in epithelia. *Nat. Rev. Mol. Cell. Biol.* 6:233–247. <http://dx.doi.org/10.1038/nrm1593>.
 12. Eisenberg S, Shvartsman DE, Ehrlich M, Henis YI. 2006. Clustering of raft-associated proteins in the external membrane leaflet modulates internal leaflet H-ras diffusion and signaling. *Mol. Cell. Biol.* 26:7190–7200. <http://dx.doi.org/10.1128/MCB.01059-06>.
 13. Johnson CM, Chichili GR, Rodgers W. 2008. Compartmentalization of phosphatidylinositol 4,5-bisphosphate signaling evidenced using targeted phosphatases. *J. Biol. Chem.* 283:29920–29928. <http://dx.doi.org/10.1074/jbc.M805921200>.
 14. Kundu A, Avalos RT, Sanderson CM, Nayak DP. 1996. Transmembrane domain of influenza virus neuraminidase, a type II protein, possesses an apical sorting signal in polarized MDCK cells. *J. Virol.* 70:6508–6515.
 15. Simons K, Ikonen E. 1997. Functional rafts in cell membranes. *Nature* 387:569–572. <http://dx.doi.org/10.1038/42408>.
 16. Keller P, Simons K. 1998. Cholesterol is required for surface transport of influenza virus hemagglutinin. *J. Cell Biol.* 140:1357–1367. <http://dx.doi.org/10.1083/jcb.140.6.1357>.
 17. Paladino S, Sarnataro D, Pillich R, Tivodar S, Nitsch L, Zurzolo C. 2004. Protein oligomerization modulates raft partitioning and apical sorting of GPI-anchored proteins. *J. Cell Biol.* 167:699–709. <http://dx.doi.org/10.1083/jcb.200407094>.
 18. Ali A, Avalos RT, Ponimaskin E, Nayak DP. 2000. Influenza virus assembly: effect of influenza virus glycoproteins on the membrane association of M1 protein. *J. Virol.* 74:8709–8719. <http://dx.doi.org/10.1128/JVI.74.18.8709-8719.2000>.
 19. Noton SL, Medcalf E, Fisher D, Mullin AE, Elton D, Digard P. 2007. Identification of the domains of the influenza A virus M1 matrix protein required for NP binding, oligomerization and incorporation into virions. *J. Gen. Virol.* 88:2280–2290. <http://dx.doi.org/10.1099/vir.0.82809-0>.
 20. Chen BJ, Leser GP, Jackson D, Lamb RA. 2008. The influenza virus M2 protein cytoplasmic tail interacts with the M1 protein and influences virus assembly at the site of virus budding. *J. Virol.* 82:10059–10070. <http://dx.doi.org/10.1128/JVI.01184-08>.
 21. Neumann G, Watanabe T, Ito H, Watanabe S, Goto H, Gao P, Hughes M, Perez DR, Donis R, Hoffmann E, Hobom G, Kawaoka Y. 1999. Generation of influenza A viruses entirely from cloned cDNAs. *Proc. Natl. Acad. Sci. U. S. A.* 96:9345–9350. <http://dx.doi.org/10.1073/pnas.96.16.9345>.
 22. Jin H, Leser GP, Lamb RA. 1994. The influenza virus hemagglutinin cytoplasmic tail is not essential for virus assembly or infectivity. *EMBO J.* 13:5504–5515.
 23. Garcia-Sastre A, Palese P. 1995. The cytoplasmic tail of the neuraminidase protein of influenza A virus does not play an important role in the packaging of this protein into viral envelopes. *Virus Res.* 37:37–47. [http://dx.doi.org/10.1016/0168-1702\(95\)00017-K](http://dx.doi.org/10.1016/0168-1702(95)00017-K).
 24. Ohkura T, Kikuchi Y, Kono N, Itamura S, Komase K, Momose F, Morikawa Y. 2012. Epitope mapping of neutralizing monoclonal antibody in avian influenza A H5N1 virus hemagglutinin. *Biochem. Biophys. Res. Commun.* 418:38–43. <http://dx.doi.org/10.1016/j.bbrc.2011.12.108>.
 25. Watanabe K, Takizawa N, Noda S, Tsukahara F, Maru Y, Kobayashi N. 2008. Hsc70 regulates the nuclear export but not the import of influenza viral RNP: a possible target for the development of anti-influenza virus drugs. *Drug Discov. Ther.* 4:77–84.
 26. Momose F, Kikuchi Y, Komase K, Morikawa Y. 2007. Visualization of microtubule-mediated transport of influenza viral progeny ribonucleoprotein. *Microbes Infect.* 9:1422–1433. <http://dx.doi.org/10.1016/j.micinf.2007.07.007>.
 27. Abramoff MD, Magelhaes PJ, Ram SJ. 2004. Image processing with ImageJ. *Biophotonics Int.* 11:36–42.
 28. Allalou A, Wahlby C. 2009. BlobFinder, a tool for fluorescence microscopy image cytometry. *Comput. Methods Programs Biomed.* 94:58–65. <http://dx.doi.org/10.1016/j.cmpb.2008.08.006>.
 29. Gu F, Crump CM, Thomas G. 2001. Trans-Golgi network sorting. *Cell. Mol. Life Sci.* 58:1067–1084. <http://dx.doi.org/10.1007/PL00000922>.
 30. Bonilha VL, Marmorstein AD, Cohen-Gould L, Rodriguez-Boulan E. 1997. Apical sorting of influenza hemagglutinin by transcytosis in retinal pigment epithelium. *J. Cell Sci.* 110:1717–1727.
 31. Gravotta D, Adesnik M, Sabatini DD. 1990. Transport of influenza HA from the trans-Golgi network to the apical surface of MDCK cells permeabilized in their basolateral plasma membranes: energy dependence and involvement of GTP-binding proteins. *J. Cell Biol.* 111:2893–2908. <http://dx.doi.org/10.1083/jcb.111.6.2893>.
 32. Wang S, Li H, Chen Y, Wei H, Gao GF, Liu H, Huang S, Chen JL. 2012. Transport of influenza virus neuraminidase (NA) to host cell surface is regulated by ARHGAP21 and Cdc42 proteins. *J. Biol. Chem.* 287:9804–9816. <http://dx.doi.org/10.1074/jbc.M111.312959>.
 33. Henkel JR, Weisz OA. 1998. Influenza virus M2 protein slows traffic along the secretory pathway. pH perturbation of acidified compartments affects early Golgi transport steps. *J. Biol. Chem.* 273:6518–6524. <http://dx.doi.org/10.1074/jbc.273.11.6518>.
 34. Bui M, Whittaker G, Helenius A. 1996. Effect of M1 protein and low pH on nuclear transport of influenza virus ribonucleoproteins. *J. Virol.* 70:8391–8401.
 35. Henkel JR, Gibson GA, Poland PA, Ellis MA, Hughey RP, Weisz OA. 2000. Influenza M2 proton channel activity selectively inhibits trans-Golgi network release of apical membrane and secreted proteins in polarized Madin-Darby canine kidney cells. *J. Cell Biol.* 148:495–504. <http://dx.doi.org/10.1083/jcb.148.3.495>.
 36. Brown DA, Rose JK. 1992. Sorting of GPI-anchored proteins to glycolipid-enriched membrane subdomains during transport to the apical cell surface. *Cell* 68:533–544. [http://dx.doi.org/10.1016/0092-8674\(92\)90189-J](http://dx.doi.org/10.1016/0092-8674(92)90189-J).
 37. Griffiths G, Simons K. 1986. The trans Golgi network: sorting at the exit site of the Golgi complex. *Science* 234:438–443. <http://dx.doi.org/10.1126/science.2945253>.
 38. Ang AL, Taguchi T, Francis S, Folsch H, Murrells LJ, Pypaert M, Warren G, Mellman I. 2004. Recycling endosomes can serve as intermediates during transport from the Golgi to the plasma membrane of MDCK cells. *J. Cell Biol.* 167:531–543. <http://dx.doi.org/10.1083/jcb.200408165>.
 39. Schuck S, Simons K. 2004. Polarized sorting in epithelial cells: raft clustering and the biogenesis of the apical membrane. *J. Cell Sci.* 117:5955–5964. <http://dx.doi.org/10.1242/jcs.01596>.
 40. Paladino S, Pocard T, Catino MA, Zurzolo C. 2006. GPI-anchored proteins are directly targeted to the apical surface in fully polarized MDCK cells. *J. Cell Biol.* 172:1023–1034. <http://dx.doi.org/10.1083/jcb.200507116>.
 41. Barman S, Adhikary L, Chakrabarti AK, Bernas C, Kawaoka Y, Nayak DP. 2004. Role of transmembrane domain and cytoplasmic tail amino acid sequences of influenza A virus neuraminidase in raft association and virus budding. *J. Virol.* 78:5258–5269. <http://dx.doi.org/10.1128/JVI.78.10.5258-5269.2004>.
 42. Jin H, Leser GP, Zhang J, Lamb RA. 1997. Influenza virus hemagglutinin and neuraminidase cytoplasmic tails control particle shape. *EMBO J.* 16:1236–1247. <http://dx.doi.org/10.1093/emboj/16.6.1236>.
 43. Yeaman C, Le Gall AH, Baldwin AN, Monlauzeur L, Le Bivic A, Rodriguez-Boulan E. 1997. The O-glycosylated stalk domain is required for apical sorting of neurotrophin receptors in polarized MDCK cells. *J. Cell Biol.* 139:929–940. <http://dx.doi.org/10.1083/jcb.139.4.929>.
 44. Razani B, Woodman SE, Lisanti MP. 2002. Caveolae: from cell biology to animal physiology. *Pharmacol. Rev.* 54:431–467. <http://dx.doi.org/10.1124/pr.54.3.431>.
 45. Schmidt U, Weiss M. 2010. Hydrophobic mismatch-induced clustering as a primer for protein sorting in the secretory pathway. *Biophys. Chem.* 151:34–38. <http://dx.doi.org/10.1016/j.bpc.2010.04.009>.
 46. Hogue IB, Grover JR, Soheilian F, Nagashima K, Ono A. 2011. Gag

- induces the coalescence of clustered lipid rafts and tetraspanin-enriched microdomains at HIV-1 assembly sites on the plasma membrane. *J. Virol.* 85:9749–9766. <http://dx.doi.org/10.1128/JVI.00743-11>.
47. Sowa G, Pypaert M, Sessa WC. 2001. Distinction between signaling mechanisms in lipid rafts vs. caveolae. *Proc. Natl. Acad. Sci. U. S. A.* 98:14072–14077. <http://dx.doi.org/10.1073/pnas.241409998>.
 48. Echarri A, Muriel O, Del Pozo MA. 2007. Intracellular trafficking of raft/caveolae domains: insights from integrin signaling. *Semin. Cell Dev. Biol.* 18:627–637. <http://dx.doi.org/10.1016/j.semcdb.2007.08.004>.
 49. Puertollano R, Martin-Belmonte F, Millan J, de Marco MC, Albar JP, Kremer L, Alonso MA. 1999. The MAL proteolipid is necessary for normal apical transport and accurate sorting of the influenza virus hemagglutinin in Madin-Darby canine kidney cells. *J. Cell Biol.* 145:141–151. <http://dx.doi.org/10.1083/jcb.145.1.141>.
 50. Tall RD, Alonso MA, Roth MG. 2003. Features of influenza HA required for apical sorting differ from those required for association with DRMs or MAL. *Traffic* 4:838–849. <http://dx.doi.org/10.1046/j.1398-9219.2003.0138.x>.
 51. Cresawn KO, Potter BA, Oztan A, Guerriero CJ, Ihrke G, Goldenring JR, Apodaca G, Weisz OA. 2007. Differential involvement of endocytic compartments in the biosynthetic traffic of apical proteins. *EMBO J.* 26:3737–3748. <http://dx.doi.org/10.1038/sj.emboj.7601813>.
 52. Scheiffele P, Rietveld A, Wilk T, Simons K. 1999. Influenza viruses select ordered lipid domains during budding from the plasma membrane. *J. Biol. Chem.* 274:2038–2044. <http://dx.doi.org/10.1074/jbc.274.4.2038>.
 53. Rayner JC, Pelham HR. 1997. Transmembrane domain-dependent sorting of proteins to the ER and plasma membrane in yeast. *EMBO J.* 16:1832–1841. <http://dx.doi.org/10.1093/emboj/16.8.1832>.
 54. Levine TP, Wiggins CA, Munro S. 2000. Inositol phosphorylceramide synthase is located in the Golgi apparatus of *Saccharomyces cerevisiae*. *Mol. Biol. Cell* 11:2267–2281. <http://dx.doi.org/10.1091/mbc.11.7.2267>.
 55. Vidal A, McIntosh TJ. 2005. Transbilayer peptide sorting between raft and nonraft bilayers: comparisons of detergent extraction and confocal microscopy. *Biophys. J.* 89:1102–1108. <http://dx.doi.org/10.1529/biophysj.105.062380>.
 56. Kaiser HJ, Orłowski A, Rog T, Nyholm TK, Chai W, Feizi T, Lingwood D, Vattulainen I, Simons K. 2011. Lateral sorting in model membranes by cholesterol-mediated hydrophobic matching. *Proc. Natl. Acad. Sci. U. S. A.* 108:16628–16633. <http://dx.doi.org/10.1073/pnas.1103742108>.
 57. Fantini J, Barrantes FJ. 2013. How cholesterol interacts with membrane proteins: an exploration of cholesterol-binding sites including CRAC, CARC, and tilted domains. *Front. Physiol.* 4:31. <http://dx.doi.org/10.3389/fphys.2013.00031>.
 58. Hanson MA, Cherezov V, Griffith MT, Roth CB, Jaakola VP, Chien EY, Velasquez J, Kuhn P, Stevens RC. 2008. A specific cholesterol binding site is established by the 2.8 Å structure of the human beta2-adrenergic receptor. *Structure* 16:897–905. <http://dx.doi.org/10.1016/j.str.2008.05.001>.
 59. Simpson DA, Lamb RA. 1992. Alterations to influenza virus hemagglutinin cytoplasmic tail modulate virus infectivity. *J. Virol.* 66:790–803.

Amino Acid Substitutions in PB1 of Avian Influenza Viruses Influence Pathogenicity and Transmissibility in Chickens

Yasushi Suzuki, Yuko Uchida, Taichiro Tanikawa, Naohiro Maeda, Nobuhiro Takemae and Takehiko Saito
J. Virol. 2014, 88(19):11130. DOI: 10.1128/JVI.01564-14.
Published Ahead of Print 16 July 2014.

Updated information and services can be found at:
<http://jvi.asm.org/content/88/19/11130>

These include:

REFERENCES

This article cites 43 articles, 24 of which can be accessed free at: <http://jvi.asm.org/content/88/19/11130#ref-list-1>

CONTENT ALERTS

Receive: RSS Feeds, eTOCs, free email alerts (when new articles cite this article), [more»](#)

Information about commercial reprint orders: <http://journals.asm.org/site/misc/reprints.xhtml>
To subscribe to to another ASM Journal go to: <http://journals.asm.org/site/subscriptions/>

Amino Acid Substitutions in PB1 of Avian Influenza Viruses Influence Pathogenicity and Transmissibility in Chickens

Yasushi Suzuki,^{a*} Yuko Uchida,^{a,b} Taichiro Tanikawa,^a Naohiro Maeda,^a Nobuhiro Takemae,^{a,b} Takehiko Saito^{a,b}

Influenza and Prion Disease Research Center, National Institute of Animal Health, National Agriculture and Food Research Organization (NARO), Tsukuba, Ibaraki, Japan^a; Zoonotic Diseases Collaboration Center (ZDCC), Chatuchak, Bangkok, Thailand^b

ABSTRACT

Amino acid substitutions were introduced into avian influenza virus PB1 in order to characterize the interaction between polymerase activity and pathogenicity. Previously, we used recombinant viruses containing the hemagglutinin (HA) and neuraminidase (NA) genes from the highly pathogenic avian influenza virus (HPAIV) H5N1 strain and other internal genes from two low-pathogenicity avian influenza viruses isolated from chicken and wild-bird hosts (LP and WB, respectively) to demonstrate that the pathogenicity of highly pathogenic avian influenza viruses (HPAIVs) of subtype H5N1 in chickens is regulated by the PB1 gene (Y. Uchida et al., *J. Virol.* 86:2686–2695, 2012, doi:<http://dx.doi.org/10.1128/JVI.06374-11>). In the present study, we introduced a C38Y substitution into WB PB1 and demonstrated that this substitution increased both polymerase activity in DF-1 cells *in vitro* and the pathogenicity of the recombinant viruses in chickens. The V14A substitution in LP PB1 reduced polymerase activity but did not affect pathogenicity in chickens. Interestingly, the V14A substitution reduced viral shedding and transmissibility. These studies demonstrate that increased polymerase activity correlates directly with enhanced pathogenicity, while decreased polymerase activity does not always correlate with pathogenicity and requires further analysis.

IMPORTANCE

We identified 2 novel amino acid substitutions in the avian influenza virus PB1 gene that affect the characteristics of highly pathogenic avian influenza viruses (HPAIVs) of the H5N1 subtype, such as viral replication and polymerase activity *in vitro* and pathogenicity and transmissibility in chickens. An amino acid substitution at residue 38 in PB1 directly affected pathogenicity in chickens and was associated with changes in polymerase activity *in vitro*. A substitution at residue 14 reduced polymerase activity *in vitro*, while its effects on pathogenicity and transmissibility depended on the constellation of internal genes.

Influenza A virus is a negative-strand RNA virus with a genome composed of eight segments. Viral subtypes are based on two surface glycoproteins, hemagglutinin (HA) and neuraminidase (NA). To date, 16 HA subtypes (H1 to H16) and 9 NA subtypes (N1 to N9) have been identified in wild birds (1, 2). Wild waterfowl are a natural host of influenza A viruses and serve as an asymptomatic reservoir.

In poultry, only a small proportion of avian influenza viruses (AIVs) are recognized as highly pathogenic avian influenza viruses (HPAIVs) on the basis of their lethality for chickens. Multiple basic amino acids at the HA cleavage sites of the H5 and H7 subtypes represent one of the molecular signatures of HPAIV (3–5). In addition to the HA cleavage site, the pathogenicity of influenza viruses is also affected by components of the viral polymerase complex, consisting of polymerase basic protein 2 (PB2), polymerase basic protein 1 (PB1), and polymerase acidic protein (PA). Reverse genetics of influenza viruses has been used to engineer recombinant viruses with targeted amino acid substitutions and to examine their effects on the pathogenicity of HPAIVs. Amino acid substitutions S224P and N383D in the PA of an H5N1 HPAIV have been found to increase polymerase activity in duck fibroblasts, coinciding with enhanced pathogenicity in ducks (6). The T515A substitution in the PA of another H5N1 HPAIV resulted in a loss of pathogenicity in ducks when the virus was inoculated orally and reduced polymerase activity *in vitro* (7). The T552S substitution in an H2N1 subtype AIV enhanced viral growth and increased polymerase activity in mammalian cells (8). The amino acid residue at position 627 in PB2 has been recognized

as an important determinant of host range for influenza A viruses. Viruses derived from avian hosts have a glutamic acid (627E) at this position, whereas a lysine (627K) is predominant at this position in human isolates (9). Enhanced polymerase activity has been shown to correlate with residue 627K in mammalian cells, and both pathogenicity and mortality were increased in mice (10–12). The Y436H substitution in the PB1 of an H5N1 HPAIV resulted in a loss of pathogenicity in ducks and reduced polymerase activity *in vitro* (7). Other substitutions in H5N1 HPAIV PB1, such as V473L and P598L, reduced plaque size in Madin-Darby canine kidney (MDCK) cells and decreased viral titers in lungs and tracheas collected from infected mice (13). Both substitutions reduced polymerase activity *in vitro* (13). The K207R substitution in the PB1 of an H5N1 virus was found to decrease polymerase activity without affecting the mortality of infected mallards and mice (7). The K480R substitution in the PB1 of an A(H1N1)pdm09 virus did not affect viral replication in MDCK cells, although it

Received 2 June 2014 Accepted 3 July 2014

Published ahead of print 16 July 2014

Editor: D. S. Lyles

Address correspondence to Takehiko Saito, taksaito@affrc.go.jp.

* Present address: Yasushi Suzuki, Influenza Virus Research Center, National Institute of Infectious Diseases, Musashimurayama, Tokyo, Japan.

Copyright © 2014, American Society for Microbiology. All Rights Reserved.

doi:10.1128/JVI.01564-14

TABLE 1 Functional consequences of amino acid substitutions in this study^a

Substitution	Effect ^a in:			
	DF-1 cells		Chickens	
	Viral replication	Polymerase activity	Pathogenicity	Transmissibility
WB → WB(L/PB1)	Up*	Up**	Up	—
LP → LP(W/PB1)	Down*	Down**	Down	—
WB → WB-PB1-C38Y	No change	Up**	Up*	—
LP(W/PB1) → LP(W/PB1-C38Y)	Up*	Up**	Up**	—
LP → LP-PB1-Y38C	—	Down**	Down*	Lost
LP → LP-PB1-V14A	No change	Down**	No change	Lost
WB(L/PB1) → WB(L/PB1-V14A)	Down*	Down**	Down ^b	No change

^a Up, increased by the substitution; Down, decreased by the substitution; —, data not applicable; Lost, lost transmissibility by substitution. For details, see Results. Statistically significant differences were observed in each category (*, $P < 0.05$; **, $P < 0.01$).

^b Viral titers in some organs were significantly decreased.

increased polymerase activity slightly in both mammalian and avian cells *in vitro* (14).

Previously, we constructed recombinant viruses possessing HA and NA genes from an H5N1 HPAIV strain (15). The internal genes were derived from two different AIVs of low pathogenicity in chickens: A/whistling swan/Shimane/580/2002 (H5N3) (WB) and A/chicken/Yokohama/aq55/2001 (H9N2) (LP) (15). When WB PB1 was replaced with LP PB1 to produce the WB(L/PB1) construct, the mean survival time (MST) was shortened from 3.33 to 2 days postinfection (dpi). WB PB1 showed the opposite effect when it was substituted for LP PB1 to construct LP(W/PB1). The MST with LP(W/PB1) was extended to 7.5 dpi, and the survival rate was increased from 6.7% to 50%. These results indicate that changes in PB1 alter the pathogenicity of the recombinant viruses in chickens, despite the presence of the same surface antigen genes as those in HPAIVs.

In this study, we compared amino acid substitutions in WB PB1 with those in LP PB1 and identified substitutions that affect polymerase activity by performing *in vitro* polymerase assays. Recombinant viruses with the substitutions described below were constructed for experimental infections in chickens. Through these analyses, we demonstrate that the C38Y substitution in PB1 consistently increased viral replication and polymerase activity *in vitro*, as well as pathogenicity in chickens. However, the V14A substitution showed variable effects on *in vitro* polymerase activity and pathogenicity or transmissibility in chickens, depending on the genetic background (Table 1).

MATERIALS AND METHODS

Viruses and cells. In this study, we used three viruses: an H5N1 subtype HPAIV (A/chicken/Yamaguchi/7/2004 [HP]) (16), a low-pathogenicity AIV of the H5N3 subtype (A/whistling swan/Shimane/580/2002; kindly provided by T. Ito, Tottori University) (WB), and an H9N2 subtype virus (A/chicken/Yokohama/aq55/2001) (LP) (17).

293T cells and DF-1 cells (a chicken fibroblast-derived cell line [CRL-12203] obtained from the American Type Culture Collection, Manassas, VA) (18) were cultured in Dulbecco's modified Eagle medium supplemented with 10% fetal calf serum and 1% penicillin-streptomycin (10,000 U/ml penicillin; 10,000 µg/ml streptomycin). MDCK cells were cultured in minimum essential medium (MEM) supplemented with 10% fetal calf serum, 1% penicillin-streptomycin, and amphotericin B (Fungizone; 2.5 µg/ml). DF-1 cells were maintained at 39°C under 5% CO₂. MDCK and 293T cells were maintained at 37°C under 5% CO₂.

Plasmid construction. Surface genes (HA and NA) were from HP, and internal genes (PB2, PB1, PA, nucleoprotein [NP], matrix protein

[M], and nonstructural protein [NS]) were from A/whistling swan/Shimane/580/2002 or A/chicken/Yokohama/aq55/2001. Segments were inserted into a pHW2000 expression vector (kindly provided by E. Hoffmann, G. Neumann, Y. Kawaoka, G. Hobom, and R. G. Webster, St. Jude Children's Research Hospital, Memphis, TN) (19) as described previously (15). Mutations were introduced by site-directed mutagenesis with the PrimeSTAR mutagenesis basal kit (TaKaRa, Shiga, Japan) according to the manufacturer's protocol and were confirmed by sequencing. The pPoll-Luc-RT plasmid, in which the human polymerase I (Pol I) promoter sequence was replaced with a chicken-derived Pol I promoter, was used for luciferase reporter assays (kindly provided by Leo L. M. Poon, University of Hong Kong, Hong Kong SAR, China) (20).

Luciferase assay of polymerase activity in DF-1 cells. Plasmid pPoll-Luc-RT and pHW2000 plasmid constructs expressing PB2, PB1, PA, or NP were cotransfected into DF-1 cells with pGL4.74 (Promega, Madison, WI) by using the TransIT-LT1 transfection reagent (Mirus, Madison, WI) as recommended by the manufacturer. Twenty-four hours after transfection at 39°C under 5% CO₂, cell extracts were collected, and luciferase activity assays were conducted with the Dual-Luciferase reporter assay system (Promega). The assay results were normalized to the activity of *Renilla* luciferase, encoded by pGL4.74.

Generation of recombinant viruses. Recombinant viruses were generated by use of a reverse genetics system (19). Equal amounts of the eight plasmid genes (PB2, PB1, PA, HA, NP, NA, M, and NS) inserted into pHW2000 were transfected into 293T cells by using the TransIT-LT1 transfection reagent (Mirus) as recommended by the manufacturer. After 48 h, supernatants were collected and were used to inoculate MDCK cells in infection medium (MEM supplemented with 0.4% bovine serum albumin, 1% penicillin-streptomycin [10,000 U/ml penicillin and 10,000 µg/ml streptomycin], amphotericin B [2.5 µg/ml], and 3% MEM vitamin solution) in order to propagate the recombinant viruses. Supernatants were harvested following the observation of cytopathic effects and were titrated to determine a 50% egg infective dose (EID₅₀) by the Reed-Muench method (21). Recombinant viruses with the HA gene from HP were handled in the biosafety level-3 facilities at the National Institute of Animal Health, Tsukuba, Japan.

Viral kinetics *in vivo*. DF-1 cells in 6-well plates (1 × 10⁶ cells/well) were infected with 0.001 EID₅₀/cell of recombinant viruses, and supernatants were collected at 24, 48, and 72 h postinfection (hpi) and were stored at -80°C. Tenfold serially diluted supernatants were inoculated into embryonated chicken eggs in order to calculate the EID₅₀. Welch's *t* test was conducted at each time point for statistical analysis of viral titers.

Animal experiments. Four-week-old specific-pathogen-free White Leghorn L-M-6 chickens were obtained from Nisseiken Co., Ltd. (Tokyo, Japan). To determine pathogenicity, chickens were inoculated intranasally with viruses at 10⁶ EID₅₀/100 µl, and survival rates were recorded for 10 days. To observe the efficiency of viral transmission, 1 of the inoc-

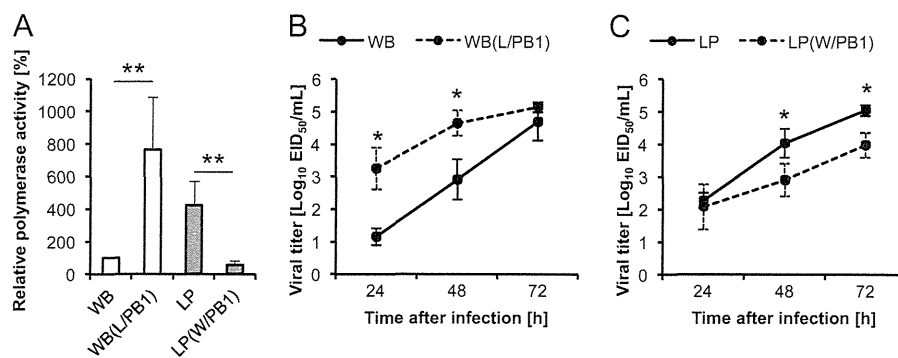


FIG 1 Polymerase activities of recombinant vRNPs generated from DF-1 cells (A) and kinetics of virus multiplication in DF-1 cells (B and C). (A) Polymerase activities (means \pm standard deviations from six or more independent experiments) of recombinant vRNPs in DF-1 cells incubated at 39°C were measured in luciferase reporter assays. The polymerase activity of WB was set at 100% as a reference. Double asterisks indicate P values of <0.01 . (B and C) Following infection of DF-1 cells with 0.001 EID₅₀/cell, supernatants were collected at 24 hpi, 48 hpi, and 72 hpi, and viral titers of WB and WB(L/PB1) (B) and of LP and LP(W/PB1) (C) were determined. Data are means \pm standard deviations at each time point (n , 3 replicates). Values were analyzed by Welch's t test. Single asterisks indicate P values of <0.05 .

ulated chickens and 3 naïve chickens were placed in the same isolator at 24 hpi. Observation lasted for 10 days from the date of initiation of cohabitation. Inoculated and naïve chickens shared feed and water. All animal experiments were conducted in the biosafety level-3 animal facilities at the National Institute of Animal Health, Tsukuba, Japan. The experimental procedures and care of the animals were approved by the Animal Experiment Committee of the National Institute of Animal Health, Tsukuba, Japan.

Survival analysis. Survival rates and periods were plotted as Kaplan-Meier survival curves (22). Survival analysis was conducted using the results of this study together with our previous results (15). Differences between recombinant and parental viruses were analyzed by a log rank test.

Titration of viruses in specimens from infected chickens. Tracheal and cloacal swab specimens were collected at 3, 5, 7, and 10 dpi and upon the death of the chickens. Swabs were dipped into transport medium (MEM containing 0.5% bovine serum-free albumin, 25 μ g/ml of amphotericin B, 1,000 U/ml of penicillin, 1,000 μ g/ml of streptomycin, 0.01 M HEPES, and 8.8 mg/ml of NaHCO₃). Organ, tracheal, and cloacal swab specimens were collected from infected chickens at 24 hpi. Swabs were dipped into transport medium, and organs were homogenized in transport medium using a Precellys 24 tissue homogenizer (Bertin Technologies, Paris, France). Swabs were removed from transport medium, and homogenized specimens were stored at -80°C until titration. Tenfold serially diluted specimens were inoculated into embryonated chicken eggs in order to calculate the EID₅₀. Welch's t tests were conducted for statistical analysis of viral titers at each time point and for the determination of differences in the tissue tropisms of recombinants.

RESULTS

Exchange of the PB1 gene between WB and LP reassortants affected polymerase activity and viral growth in DF-1 cells. First, to examine whether exchanging the PB1 gene affects the polymerase activity of reassortants, the polymerase activities of recombinant viral ribonucleoproteins (vRNPs) were measured by a luciferase reporter assay in DF-1 cells *in vitro* (Fig. 1A). The polymerase activity of WB(L/PB1) showed an 8-fold increase over that of WB ($P < 0.01$), and the MST was shortened by 1.33 days. In contrast, the polymerase activity of LP(W/PB1) showed a 7-fold decrease in activity from that of LP ($P < 0.01$) and a longer MST than that with LP.

Next, we examined the growth kinetics of WB and WB(L/PB1) and of LP and LP(W/PB1) *in vitro* in order to see whether the

changes observed in polymerase activity affected the growth of viruses in DF-1 cells (Fig. 1B and C). WB(L/PB1) grew more rapidly than WB until 48 hpi, and the viral titers of WB(L/PB1) were significantly higher than those of WB at 24 hpi and 48 hpi ($P < 0.05$) (Fig. 1B). There was no significant difference in titers between WB(L/PB1) and WB at 72 hpi. However, growth deceleration of LP(W/PB1) was observed after 48 hpi (Fig. 1C). The viral titers of LP(W/PB1) were significantly lower than those of LP at 48 hpi and 72 hpi ($P < 0.05$), although there were no significant differences at 24 hpi. These results suggested that the PB1 gene of WB is involved in the lower polymerase activity and lower growth rates of WB and LP(W/PB1) than of LP.

Contribution of the C38Y substitution in WB PB1 to enhanced polymerase activity and viral growth. Twenty amino acid differences were found between the PB1 sequences of WB and LP (Table 2). To identify the residue(s) responsible for differences in polymerase activity, we selected 7 amino acid residues, at positions 14, 38, 52, 171, 211, 398, and 739, for a site-directed mutagenesis study. The residues at positions 14 and 739 are located in the binding domains for PA and PB2 (23, 24), and the other five substitutions are relatively unique to WB PB1 among AIVs (Table 2). The amino acid residue at each selected site in WB PB1 was changed to the corresponding residue found in LP PB1, and vice versa.

In WB, a cysteine-to-tyrosine substitution at residue 38 (C38Y) of PB1 resulted in higher polymerase activity than that of wild-type WB PB1 ($P < 0.01$) (Fig. 2A). No significant increase in polymerase activity was observed following substitutions of the other 6 amino acids (Fig. 2A). The effects of C38Y in WB PB1 were also observed when WB-PB1-C38Y was combined with LP PB2, PA, and NP to construct LP(W/PB1-C38Y). The polymerase activity of LP(W/PB1-C38Y) was significantly higher than that of LP(W/PB1) ($P < 0.01$) (Fig. 2B). Inhibitory effects were observed when the Y38C substitution was introduced into LP PB1. The polymerase activities of WB(L/PB1-Y38C) and LP-PB1-Y38C were significantly lower than those of WB(L/PB1) and LP, respectively (Fig. 2C). Thus, the residue at position 38 is a key amino acid regulating polymerase activity in WB PB1, independently of the other components of the polymerase complex of WB or LP.

In DF-1 cells, the replication of WB-PB1-C38Y, which pos-

TABLE 2 Amino acid differences in PB1 between WB and LP, and prevalences of WB PB1 amino acid residues in viruses isolated from avian species and chickens from the NCBI Influenza Virus Resource

Amino acid position	Residue in:		No. (%) of strains encoding the same amino acid residue as that in WB ^a				
	WB	LP	H5N3 strains (n = 42)	H9N2 strains (n = 501)	H5N1 strains (n = 1,201)	Strains isolated from chickens (n = 1,226)	Strains isolated from avian species (n = 7,762)
14	A	V	39 (92.9)	269 (53.7)	144 (12.0)	445 (36.3)	6,198 (79.9)
38	C	Y	1 (2.4)	2 (0.4)	0 (0.0)	1 (0.1)	3 (0.0)
52	R	K	1 (2.4)	6 (1.2)	7 (0.6)	26 (2.1)	125 (1.6)
62	G	K	40 (95.2)	385 (76.8)	1,196 (99.6)	1,131 (92.3)	7,590 (97.8)
75	E	D	42 (100.0)	385 (76.8)	1,185 (98.7)	1,068 (87.1)	7,512 (96.8)
76	D	N	42 (100.0)	391 (78.0)	1,159 (96.5)	1,118 (91.2)	7,562 (97.4)
111	M	I	42 (100.0)	403 (80.4)	1,193 (99.3)	1,140 (93.0)	7,636 (98.4)
157	A	T	41 (97.6)	381 (76.0)	1,195 (99.5)	1,108 (90.4)	7,525 (96.9)
171	L	M	1 (2.4)	0 (0.0)	1 (0.1)	2 (0.2)	10 (0.1)
172	E	D	41 (97.6)	304 (60.7)	1,190 (99.1)	981 (80.0)	7,355 (94.8)
175	D	N	42 (100.0)	393 (78.4)	1,180 (98.3)	1,108 (90.4)	7,264 (93.6)
211	K	R	1 (2.4)	25 (5.0)	22 (1.8)	38 (3.1)	173 (2.2)
214	K	R	40 (95.2)	382 (76.2)	1,194 (99.4)	1,115 (90.9)	7,464 (96.2)
215	K	R	9 (21.4)	93 (18.6)	686 (57.1)	435 (35.5)	1,683 (21.7)
317	M	V	42 (100.0)	352 (70.3)	1,176 (97.9)	1,050 (85.6)	7,138 (92.0)
375	N	T	29 (69.0)	325 (64.9)	1,120 (93.3)	968 (79.0)	4,616 (59.5)
387	K	Q	39 (92.9)	263 (52.5)	1,156 (96.3)	949 (77.4)	7,333 (94.5)
398	N	E	3 (7.1)	5 (1.0)	3 (0.2)	6 (0.5)	26 (0.3)
621	Q	K	42 (100.0)	333 (66.5)	1,184 (98.6)	1,057 (86.2)	7,457 (96.1)
739	D	E	1 (2.4)	11 (2.2)	2 (0.2)	9 (0.7)	36 (0.5)

^a Shown are the numbers of strains that were categorized into the respective criteria extracted from the NCBI Influenza Virus Resource.

sesses WB PB1 with the C38Y substitution, did not differ significantly from that of recombinants with wild-type WB PB1 (Fig. 3A). In contrast, the viral titers of LP(W/PB1-C38Y), which possesses WB PB1 with C38Y along with the other internal genes from LP, were significantly higher than those of LP(W/PB1) at 48 hpi and 72 hpi ($P < 0.05$) (Fig. 3B).

The V14A substitution in LP PB1 reduced polymerase activity. We also examined the effects of amino acid alterations from valine to alanine at residue 14 (V14A) and from glutamic acid to aspartic acid at residue 739 (E739D) in LP PB1, because these residues are located in the PA- and PB2-binding domains of PB1. In addition, the frequency of V14 among AIVs was biased in the H5N1 and H9N2 strains (Table 2). V14A caused a significant decrease in polymerase activity when combined with the PB2, PA, and NP of LP or WB ($P < 0.01$) (Fig. 2C). E739D caused an increase in activity when combined with other components from LP ($P < 0.01$) but not when combined with other components from WB. No significant differences in viral replication were observed between LP and LP-PB1-V14A (Fig. 3C). The viral titer of WB(L/PB1-V14A) was significantly lower than that of WB(L/PB1) at 72 hpi ($P < 0.05$) (Fig. 3D).

The substitution at amino acid position 38 in the PB1 gene affected pathogenicity in chickens. Survival analysis was performed to examine the pathogenicities of recombinant viruses with the PB1 C38Y substitution in chickens. The pathogenicity of WB-PB1-C38Y was found to be higher than that of WB ($P = 0.025$) (Fig. 4A). The MST of chickens infected with WB was shortened from 3.39 dpi to 2.25 dpi by the C38Y substitution (WB-PB1-C38Y). The effect of C38Y in WB PB1 on survival was greatly enhanced ($P = 0.008$) by combination with LP PB2, PA, and NP [LP(W/PB1-C38Y)] (Fig. 4B). The survival rate of chickens infected with LP(W/PB1) was decreased from 50% to 0%, and the MST was shortened from 7.50 dpi to 3.00 dpi, by the C38Y

substitution. In a comparison of WB with WB-PB1-C38Y, no significant differences were observed between the viral titers in tracheal and cloacal swabs or in organs collected from infected chickens (Fig. 4C and E; Table 3).

The level of viral shedding at 3 dpi in tracheal swabs from LP(W/PB1-C38Y)-infected chickens was significantly higher than that observed with LP(W/PB1) (Fig. 4D). LP(W/PB1) showed the maximum viral titer at 5 dpi; however, the maximum titer in chickens infected with LP(W/PB1-C38Y) was observed at 3 dpi (Fig. 4D). Viral titers in cloacal swabs did not differ significantly between LP(W/PB1-C38Y) and LP(W/PB1) (Fig. 4F). No apparent differences in tissue tropism were observed between LP(W/PB1-C38Y) and LP(W/PB1) (Table 4).

To confirm that the Y residue at position 38 in PB1 regulates H5N1 HPAIV pathogenicity in chickens, we constructed the recombinant virus LP-PB1-Y38C, which possesses the Y38C substitution in LP PB1. We observed by survival analysis that the pathogenicity of LP-PB1-Y38C was reduced from that of LP ($P = 0.025$) (Fig. 5A). The survival rate of chickens infected with LP-PB1-Y38C was increased from 4.3% to 40%, and the MST was extended from 3.77 dpi to 6.80 dpi (Fig. 5A). Viral titers in tracheal swabs from chickens exposed to LP-PB1-Y38C were significantly lower at 3 dpi than those from chickens exposed to LP (Fig. 5B), while no significant differences were observed in cloacal swabs (Fig. 5C). The transmissibility of LP-PB1-Y38C was examined in order to determine if the decreased pathogenicity resulting from the Y38C substitution is associated with reduced transmissibility of the recombinant virus. LP-PB1-Y38C was not transmitted from infected chickens to any naïve chickens in the same isolator (see Fig. 7), and viral titers in tracheal swabs at 4 dpi did not differ from those observed with LP (Fig. 5B). Thus, both pathogenicity and transmissibility were reduced by the Y38C substitution in LP PB1.

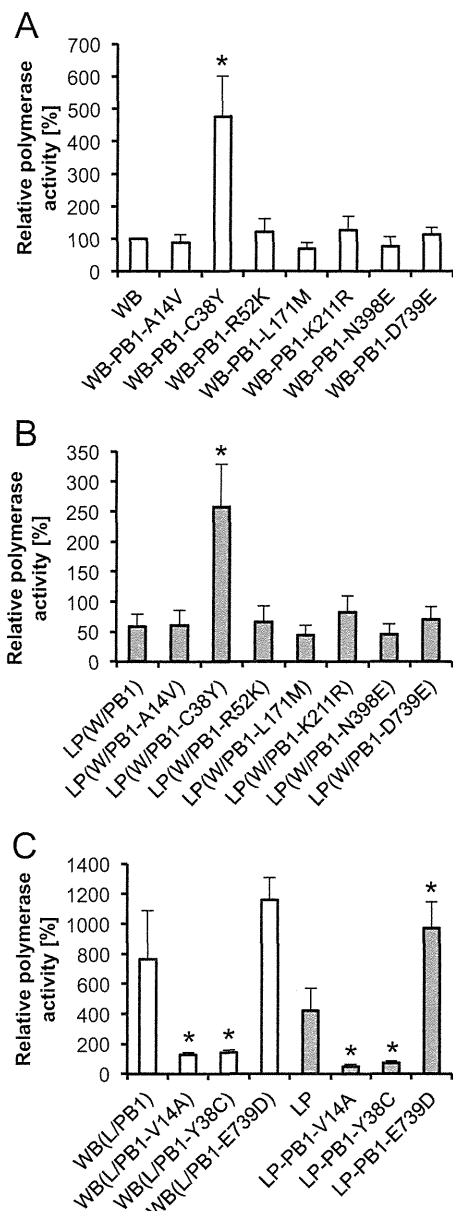


FIG 2 Effects of PB1 amino acid substitutions on polymerase activity. (A and B) The effects of 7 amino acid substitutions in WB PB1 on polymerase activity were analyzed in a WB background (A) and in an LP background (B). Asterisks indicate significant differences ($P < 0.01$) from WB (A) and from LP(W/PB1) (B). (C) Three amino acid substitutions in LP PB1 were analyzed for their effects on polymerase activity in WB and LP. Asterisks indicate significant differences among WB(L/PB1) variants in the WB background or among LP variants in the LP background ($P < 0.01$). Values are means \pm standard deviations for three or more independent experiments. Statistical differences in mean polymerase activities were assessed with Bonferroni's multiple-comparison test.

V14A in LP PB1 reduces transmissibility in chickens. To investigate the influence of the V14A substitution in LP PB1 on the pathogenicities of recombinants, survival analysis was performed comparing LP with LP-PB1-V14A and WB(L/PB1) with WB(L/PB1-V14A). Survival analysis revealed no significant difference between LP and LP-PB1-V14A ($P = 0.764$) (Fig. 6A). Similarly, there was no significant difference between WB(L/PB1) and WB(L/PB1-V14A) ($P = 0.317$) (Fig. 6B).

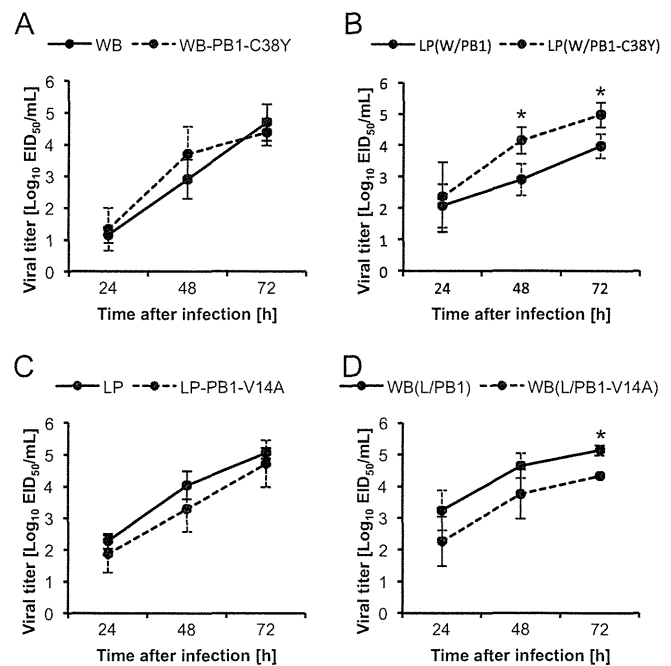


FIG 3 (A and B) Viral titers of recombinants possessing the C38Y substitution in PB1 in a WB background (A) or an LP(W/PB1) background (B). (C and D) Viral titers of recombinants possessing the V14A substitution in PB1 in an LP background (C) or a WB(L/PB1) background (D). Values are means \pm standard deviations for three replicates. Viral titers at each time point were analyzed by Welch's t test. Asterisks indicate P values of < 0.05 .

Next, we compared viral shedding and tissue distribution in chickens infected with a parental virus and those infected with a recombinant, or in chickens infected with different recombinants; LP was compared with LP-PB1-V14A, and WB(L/PB1) was compared with WB(L/PB1-V14A). The viral titers in tracheal swabs from LP-PB1-V14A-infected chickens were significantly lower at 3 dpi than those from LP-infected chickens (Fig. 6C), although no significant difference in viral titers was observed with cloacal swabs (Fig. 6E). The viral titers of LP-PB1-V14A in the lung were decreased (Table 5). A comparison of WB(L/PB1) and WB(L/PB1-V14A) showed that the level of viral shedding from tracheal swabs was significantly lower for WB(L/PB1-V14A) than for WB(L/PB1) at 1 dpi ($P < 0.05$) (Fig. 6D). There were no significant differences in viral titers in cloacal swabs (Fig. 6F). A comparison of tissue tropism in WB(L/PB1-V14A) and WB(L/PB1) showed a tendency for WB(L/PB1-V14A) titers to decline in most organs; they were significantly lower in the muscle ($P < 0.01$), liver ($P < 0.05$), trachea ($P < 0.05$), and tracheal swabs ($P < 0.05$) (Table 6) (the same data are shown for tracheal swabs in Fig. 6D).

A transmission study was conducted to evaluate the effects of the V14A substitution, which resulted in reduced polymerase activity, while no change in pathogenicity was observed. LP was transmitted to all 3 naïve chickens in the same isolator as an infected chicken by the end of the observation period; in contrast, LP-PB1-V14A was not transmitted to any naïve chickens in the same isolator (Fig. 7). Tracheal and cloacal swabs were collected at 3 dpi from inoculated chickens, and the LP titers from tracheal swabs were significantly higher than the LP-PB1-V14A titers (Fig. 6C). These results were consistent with the differences in transmissibility between LP and the recombinant LP-PB1-V14A virus

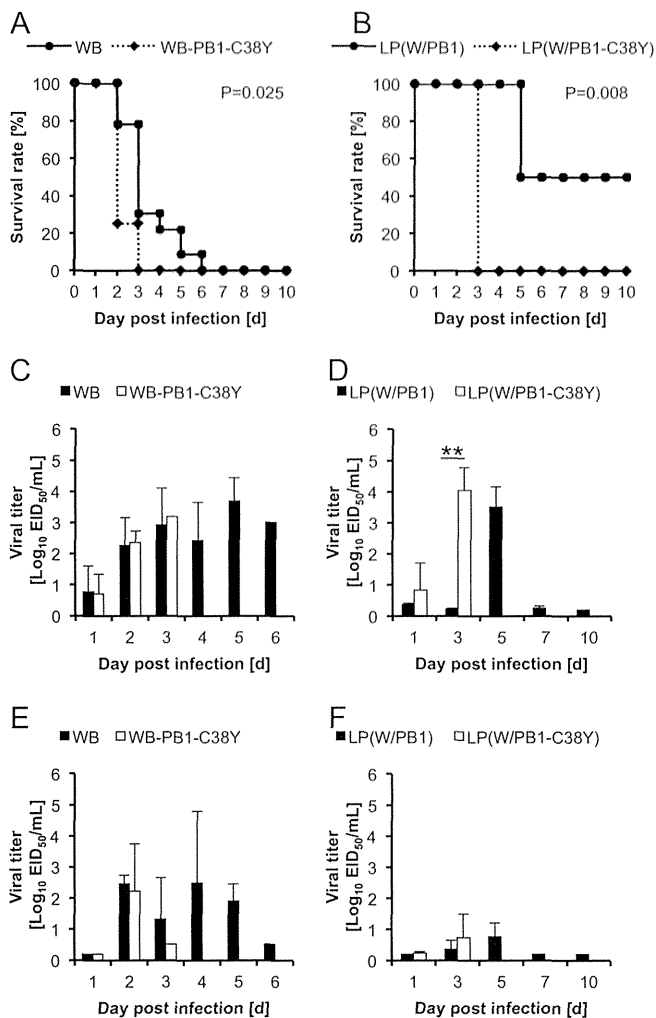


FIG 4 Pathogenicities of recombinant viruses with the C38Y substitution in WB PB1 for chickens. (A and B) Survival plots for chickens infected with WB or WB-PB1-C38Y (A) and for chickens infected with LP(W/PB1) or LP(W/PB1-C38Y) (B). The survivability of chickens ($n \geq 4$) was determined, and Kaplan-Meier survival rate curves were plotted and were analyzed by the log rank test. (C to F) Viral titers in tracheal (C and D) and cloacal (E and F) swabs from infected chickens. Swabs were taken from chickens infected with WB or WB-PB1-C38Y (C and E) and from chickens infected with LP(W/PB1) or LP(W/PB1-C38Y) (D and F) at 3, 5, 7, and 10 dpi routinely and upon the deaths of the chickens. Viral titers at 1 dpi were those obtained in the experiment reported in Tables 3 and 4. Viral titers at each time point were analyzed by Welch's t test. Double asterisks indicate a P value of <0.01 .

with reduced polymerase activity. In contrast, WB(L/PB1) was transmitted to 2 of the 3 naïve chickens, and WB(L/PB1-V14A) was transmitted to all 3 naïve chickens, during the observation period (Fig. 7). These two viruses showed nearly identical transmissibility, although the titer of WB(L/PB1-V14A) from tracheal swabs at 1 dpi was significantly lower than that of WB(L/PB1) (Fig. 6D).

DISCUSSION

In this study, we found that the C38Y substitution in WB PB1 increased both polymerase activity *in vitro* and pathogenicity in chickens. The recombinant viruses with this substitution, WB-PB1-C38Y and LP(W/PB1-C38Y), showed higher pathogenicity

TABLE 3 Viral titers in organs collected from chickens at 24 h after infection with WB or WB-PB1-C38Y

Organ or sample	Titer (\log_{10} EID ₅₀ /ml) ^a					
	WB			WB-PB1-C38Y		
	Animal 1	Animal 2	Animal 3	Animal 1	Animal 2	Animal 3
Pancreas	<1.20	3.38	<0.20	<0.20	3.20	2.53
Spleen	<1.20	3.53	<0.20	<0.20	4.20	3.20
Muscle	<1.20	3.30	<0.20	<0.20	2.20	2.20
Liver	<1.20	3.92	<0.20	0.53	3.07	3.20
Bursa of Fabricius	<1.20	<1.20	<0.20	<0.20	3.32	3.20
Trachea	<1.20	2.06	<0.20	<0.20	3.02	2.07
Lung	<1.20	5.45	<0.20	<0.20	3.07	2.20
Kidney	<1.20	3.32	<0.20	<0.20	2.53	1.70
Heart	<1.20	4.87	<0.20	<0.20	2.38	2.53
Comb	<1.20	3.38	<0.20	<0.20	3.32	2.87
Wattle	<1.20	4.07	<0.20	<0.20	3.02	2.20
Brain	<1.20	2.32	<0.20	<0.20	3.20	3.07
Duodenum	—	3.32	<0.20	<0.20	3.38	2.20
Rectum	<1.20	3.92	<0.20	<0.20	3.53	3.53
Blood	<1.20	3.30	<0.20	<0.20	1.20	1.38
Tracheal swab	<0.20	1.95	<0.20	<0.20	1.60	0.32
Cloacal swab	<0.20	<0.20	<0.20	<0.20	<0.20	<0.20

^a The detection limit was either <1.20 or <0.20 \log_{10} EID₅₀/ml. —, sample not available.

in chickens than the parental viruses WB and LP(W/PB1), respectively. Previously, a correlation was reported between enhanced polymerase activity and pathogenicity with substitutions in the PA gene of an H5N1 strain (6). A/duck/Hubei/49/05 (DK/49) showed higher polymerase activity in duck fibroblasts and higher pathogenicity in ducks than A/goose/Hubei/65/05 (GS/65). When the S224P and N383D substitutions in PA were introduced into strain GS/65, polymerase activity and pathogenicity were enhanced (6).

TABLE 4 Viral titers in organs collected from chickens at 24 h after infection with LP(W/PB1) or LP(W/PB1-C38Y)

Organ or sample	Titer (\log_{10} EID ₅₀ /ml) ^a					
	LP(W/PB1)			LP(W/PB1-C38Y)		
	Animal 1	Animal 2	Animal 3	Animal 1	Animal 2	Animal 3
Pancreas	<0.20	<0.20	<0.20	<0.20	<0.20	<0.20
Spleen	<0.20	<0.20	0.32	<0.20	<0.20	<0.20
Muscle	<0.20	<0.20	<0.20	<0.20	<0.20	<0.20
Liver	<0.20	<0.20	<0.20	0.32	<0.20	<0.20
Bursa of Fabricius	<0.20	<0.20	<0.20	<0.20	<0.20	<0.20
Trachea	<0.20	<0.20	<0.20	<0.20	0.32	<0.20
Lung	<0.20	<0.20	<0.20	<0.20	0.53	0.53
Kidney	<0.20	<0.20	<0.20	<0.20	0.32	<0.20
Heart	<0.20	<0.20	<0.20	<0.20	0.70	<0.20
Comb	0.32	<0.20	<0.20	<0.20	<0.20	<0.20
Wattle	<0.20	<0.20	<0.20	<0.20	<0.20	<0.20
Brain	0.32	<0.20	<0.20	<0.20	<0.20	<0.20
Duodenum	<0.20	<0.20	<0.20	<0.20	<0.20	<0.20
Rectum	<0.20	<0.20	<0.20	<0.20	<0.20	<0.20
Blood	<0.20	<0.20	<0.20	<0.20	<0.20	<0.20
Tracheal swab	0.32	0.45	0.30	2.07	<0.20	<0.20
Cloacal swab	<0.20	<0.20	<0.20	<0.20	<0.20	0.32

^a The detection limit was <0.20 \log_{10} EID₅₀/ml.

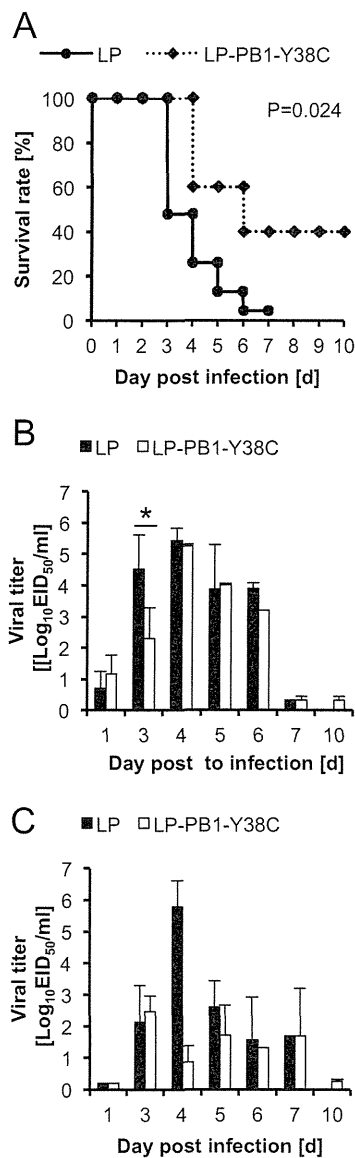


FIG 5 Pathogenicities of recombinant viruses with the Y38C substitution in LP PB1 for chickens. (A) The survivability of chickens ($n \geq 4$) was determined, and Kaplan-Meier survival rate curves were plotted and were analyzed by the log rank test. (B and C) Viral titers in tracheal (B) and cloacal (C) swabs taken from infected chickens at 1, 3, 5, 7, and 10 dpi routinely and upon the deaths of the chickens were determined. Viral titers at each time point were analyzed by Welch's t test. The asterisk indicates a P value of <0.05 .

The E627K substitution in the PB2 of an AIV was reported to increase polymerase activity in mammalian cells (10), and this substitution in an H5N1 HPAIV enhanced virulence in mice (11, 12). Higher polymerase activity was also attributed to the higher pathogenicity of A/duck/Fujian/01/2002 in mice and chickens than of A/duck/Guangxi/53/2002 (25, 26). In the present study, along with others, demonstrates that enhanced polymerase activity is a major determinant of enhanced pathogenicity.

PB1 serves a central role in the formation of the structural backbone of the viral polymerase complex and has RNA polymerase activity (27–29). In addition, PB1 has viral RNA (vRNA)-binding domains (amino acids 1 to 139, 233 to 249, and 494 to

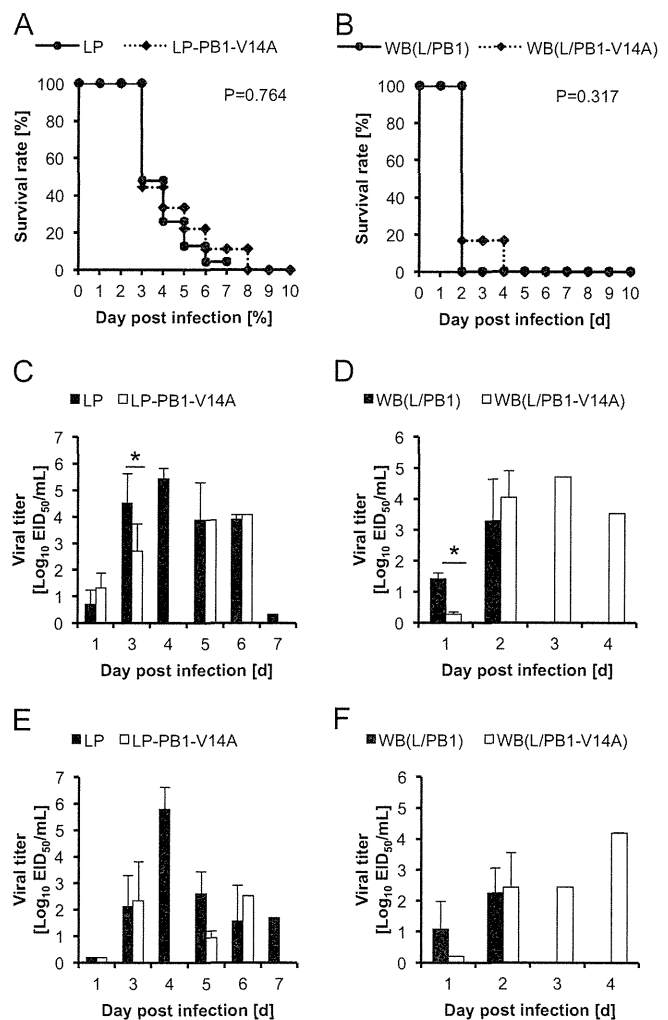


FIG 6 Pathogenicities of recombinant viruses with the V14A substitution in LP PB1 for chickens. (A and B) Survival plots for chickens infected with LP or LP-PB1-V14A (A) and for chickens infected with WB(L/PB1) or WB(L/PB1-V14A) (B). The survivability of chickens ($n \geq 4$) was determined, and Kaplan-Meier survival rate curves were plotted and were analyzed by the log rank test. (C to F) Viral titers in tracheal (C and D) and cloacal (E and F) swabs from chickens infected with LP or LP-PB1-V14A (C and E) and from chickens infected with WB(L/PB1) or WB(L/PB1-V14A) (D and F). Swabs were collected at 3, 5, 7, and 10 dpi routinely and upon the deaths of the chickens. Viral titers at 1 dpi were those obtained in the experiment reported in Tables 5 and 6. Viral titers at each time point were analyzed by Welch's t test. Asterisks indicate P values of <0.05 .

757) and cRNA-binding domains (amino acids 1 to 139 and 267 to 493) (30, 31). Although C38Y resides in both the vRNA- and cRNA-binding domains, it does not confer binding of PB1 to vRNA. Jung and Brownlee demonstrated that changes from alanine to arginine at positions 233, 238, 239, and 249 impaired vRNA, cRNA, and mRNA synthesis *in vitro* by disabling the binding activity of PB1 to the vRNA promoter (31), indicating that the essential domains for vRNA binding are located at amino acids 233 to 249. These results are consistent with a previous report demonstrating that hairpin-loop RNA bound to the arginine-rich domain (32). The polymerase function of PB1 resides in four conserved polymerase motifs (amino acids 303 to 306, 403 to 412, 438 to 450, and 474 to 484) (28, 33). V473L and P598L, at positions in

TABLE 5 Viral titers in organs collected from chickens at 24 h after infection with LP or LP-PB1-V14A

Organ or sample	Titer (\log_{10} EID ₅₀ /ml) ^a					
	LP			LP-PB1-V14A		
	Animal 1	Animal 2	Animal 3	Animal 1	Animal 2	Animal 3
Pancreas	<1.20	<1.20	<0.20	<0.20	<0.20	0.87
Spleen	<1.20	<1.20	<0.20	0.32	<0.20	<0.20
Muscle	<1.20	1.70	<0.20	<0.20	<0.20	<0.20
Liver	<1.20	<1.20	<0.20	<0.20	<0.20	<0.20
Bursa of Fabricius	<1.20	1.32	0.32	<0.20	<0.20	<0.20
Trachea	<1.20	2.45	0.32	<0.20	<0.20	1.38
Lung	1.53	3.32	<0.20	<0.20	0.32	0.32
Kidney	<1.20	2.02	0.32	<0.20	<0.20	<0.20
Heart	<1.20	2.45	<0.20	0.32	<0.20	<0.20
Comb	1.53	<1.20	<0.20	0.32	<0.20	<0.20
Wattle	<1.20	2.07	<0.20	<0.20	<0.20	<0.20
Brain	<1.20	2.02	<0.20	<0.20	<0.20	<0.20
Duodenum	<1.20	<1.20	<0.20	<0.20	<0.20	<0.20
Rectum	<1.20	<1.20	<0.20	<0.20	<0.20	<0.20
Blood	<1.20	<1.20	<0.20	<0.20	<0.20	<0.20
Tracheal swab	0.45	1.45	<0.20	0.53	1.62	1.79
Cloacal swab	<0.20	<0.20	<0.20	<0.20	<0.20	<0.20

^a The detection limit was either <1.20 or <0.20 \log_{10} EID₅₀/ml.

motif IV and near the PB2-binding domain, respectively, reduced polymerase activity (13). C38Y does not reside in either the PA-binding domain at the N terminus (amino acids 1 to 15) or the PB2-binding domain at the C terminus (amino acids 685 to 757) of PB1 (23, 24, 34). How C38Y in PB1 affects the polymerase activity needs to be elucidated by further analyses.

The alteration of viral replication by substitutions in the PB1

TABLE 6 Viral titers in organs collected from chickens at 24 h after infection with WB(L/PB1) or WB(L/PB1-V14A)

Organ or sample ^a	Titer (\log_{10} EID ₅₀ /ml) ^b					
	WB(L/PB1)			WB(L/PB1-V14A)		
	Animal 1	Animal 2	Animal 3	Animal 1	Animal 2	Animal 3
Pancreas	3.32	2.53	2.53	0.53	2.20	<0.20
Spleen	4.87	3.20	3.20	1.07	3.20	<0.20
Muscle**	3.20	2.32	2.38	<0.20	1.20	<0.20
Liver*	4.07	2.87	3.32	0.70	2.32	<0.20
Bursa of Fabricius	3.20	2.32	1.70	0.32	2.38	<0.20
Trachea*	4.02	3.53	2.87	0.32	2.32	<0.20
Lung	4.45	3.53	3.20	0.53	4.07	<0.20
Kidney	4.38	2.32	2.53	0.53	2.20	<0.20
Heart	4.53	3.20	3.32	<0.20	3.32	0.53
Comb	3.02	2.87	2.45	<0.20	3.07	<0.20
Wattle	3.20	3.20	3.20	<0.20	2.53	<0.20
Brain	3.87	3.87	2.32	<0.20	2.32	<0.20
Duodenum	3.53	2.87	2.07	0.53	2.20	<0.20
Rectum	3.87	2.20	2.20	<0.20	1.87	<0.20
Blood	1.32	0.87	0.32	<0.20	0.53	<0.20
Tracheal swab*	1.70	1.32	<0.20	<0.20	0.32	0.32
Cloacal swab	0.70	2.32	<0.20	<0.20	<0.20	<0.20

^a Asterisks indicate statistically significant differences in viral titers between WB(L/PB1) and WB(L/PB1-V14A), as determined by Welch's *t* test (*, *P* < 0.05; **, *P* < 0.01).

^b The detection limit was <0.20 \log_{10} EID₅₀/ml.

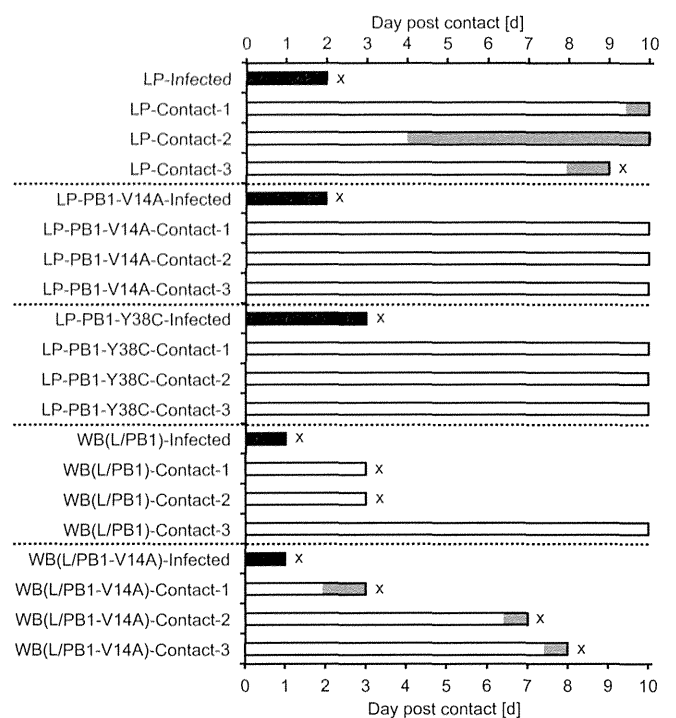


FIG 7 Transmissibilities of recombinant viruses in chickens. Filled and shaded bars indicate durations of detectable virus in tracheal and/or cloacal swabs from infected and contacted chickens, respectively. The letter "x" indicates the time point at which a chicken died from infection. Cohabitation with infected chickens started at 1 dpi.

protein was not always consistent with that of polymerase activities observed in DF-1 cells. Two critical steps must occur with viral transcripts for the replication cycle to be completed: vRNA synthesis and viral protein translation. A temperature-sensitive virus with a C-terminal deletion in the NS1 protein showed reduced vRNA levels and low infectivity at the restrictive temperature (39.5°C), while the accumulation of cRNA and mRNA was not altered (35). In addition, signaling through the nuclear factor κ B (NF- κ B) pathway, a prerequisite for efficient influenza virus infection, was activated by infection with influenza A virus (36, 37), and an NF- κ B inhibitor reduced vRNA production and viral infectivity without influencing viral mRNA levels (38). In the present study, polymerase activities were measured by luciferase assays, which reflect fluctuations in viral mRNA production but not in vRNA levels. A possible explanation of the discrepancy observed between viral replication and polymerase activities is that vRNA production may have been variably affected by mutations in PB1 residue 14 or 38, while mRNA synthesis was consistently affected, though not to an extent that would affect virus production.

LP-PB1-V14A, a recombinant virus with the V14A substitution, displayed a reduced level of viral shedding in infected chickens and lost the ability to be transmitted to naïve chickens. Virus shedding is a key factor in successful transmission between an infected and a naïve chicken, since influenza viruses are transmitted through aerosols, large droplets, or direct contact with secretions (39). Reduced polymerase activity has been shown to be associated with restricted transmissibility of HPAIVs. Hulse-Post et al. reported that reduced polymerase activity with the Y436H

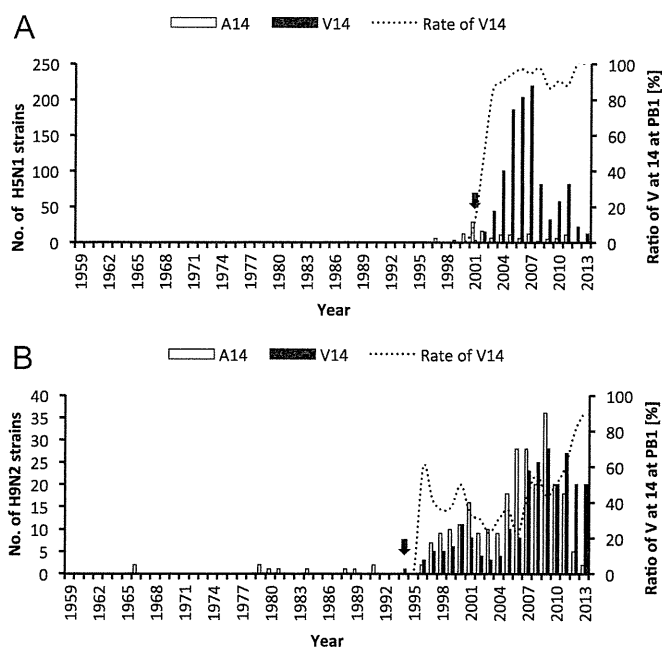


FIG 8 Numbers of strains with alanine or valine at amino acid position 14 in PB1 and percentages of H5N1 (A) and H9N2 (B) strains since 1959. Black arrows indicate when the oldest strain possessing V14 in PB1 appeared. Percentages were calculated when the number of strains of each subtype in the same year was greater than 5.

substitution in PB1 resulted in lowered transmissibility and pathogenicity in ducks (7). Lyall et al. established transgenic chickens in which the RNA polymerase activity of a polymerase complex from an AIV was hampered by expressing a short hairpin RNA as an RNA decoy (40). When these transgenic chickens were infected with an HPAIV, the efficiency of transmission of the virus to transgenic and nontransgenic chickens was reduced, although transgenic chickens were still susceptible to initial infection. The level of shedding of the virus from the cloacae of transgenic chickens was apparently lower than that in nontransgenic infected chickens. Impaired polymerase activity in LP-PB1-V14A caused reduced transmissibility of the virus without affecting its lethality. Although other causes have not been eliminated, it is likely that the reduced transmissibility of LP-PB1-V14A could be the result of reduced secretions in the trachea. The functional change resulting from the V14A substitution requires further study, considering that Perez and Donis found that A14V does not affect PA binding (41), while Wunderlich et al. demonstrated reduced binding to PA by PB1-derived peptides containing the V14A mutation (42).

It is worth considering whether the V14A substitution may play a role in the dissemination of viruses in the field, since the frequency of valine at residue 14 in PB1 is much higher in H5N1 isolates than in other AIV isolates, a majority of which possess alanine at this position (Table 2). The H5N1 and H9N2 viruses with A14V have emerged since 2001 and 1994, respectively (Fig. 8). During the initial outbreak in 1997, H5N1 viruses possessed A14, but the frequency of V14 suddenly increased in 2003, corresponding with an eruption of the viruses in Asian countries (43). In addition, V14 in H9N2 viruses was confirmed in 1994, and the population has gradually increased.

In conclusion, we found that two novel amino acid substitutions in the PB1 protein, namely, C38Y in WB PB1 and V14A in LP PB1, alter polymerase activity. Altered polymerase activity was shown to be an important factor for viral pathogenesis in chickens. C38Y contributes to an increase in polymerase activity, accompanied by a shortened MST, while V14A affects transmissibility in chickens. Although the molecular bases of the change in polymerase activity and the altered host responses induced by the changes remain to be elucidated, our results demonstrate the involvement of PB1 in the pathogenesis of HPAIV in chickens.

ACKNOWLEDGMENT

This work was supported by a Grant-in-Aid for Scientific Research from the Zoonoses Control Project of the Ministry of Agriculture, Forestry, and Fisheries of Japan.

REFERENCES

- Webster RG, Bean WJ, Gorman OT, Chambers TM, Kawaoka Y. 1992. Evolution and ecology of influenza A viruses. *Microbiol. Rev.* 56:152–179.
- Fouchier RA, Munster V, Wallensten A, Bestebroer TM, Herfst S, Smith D, Rimmelzwaan GF, Olsen B, Osterhaus AD. 2005. Characterization of a novel influenza A virus hemagglutinin subtype (H16) obtained from black-headed gulls. *J. Virol.* 79:2814–2822. <http://dx.doi.org/10.1128/JVI.79.5.2814-2822.2005>.
- Senne DA, Panigrahy B, Kawaoka Y, Pearson JE, Suss J, Lipkind M, Kida H, Webster RG. 1996. Survey of the hemagglutinin (HA) cleavage site sequence of H5 and H7 avian influenza viruses: amino acid sequence at the HA cleavage site as a marker of pathogenicity potential. *Avian Dis.* 40:425–437. <http://dx.doi.org/10.2307/1592241>.
- Horimoto T, Kawaoka Y. 1994. Reverse genetics provides direct evidence for a correlation of hemagglutinin cleavability and virulence of an avian influenza A virus. *J. Virol.* 68:3120–3128.
- Steinhauer DA. 1999. Role of hemagglutinin cleavage for the pathogenicity of influenza virus. *Virology* 258:1–20. <http://dx.doi.org/10.1006/viro.1999.9716>.
- Song J, Feng H, Xu J, Zhao D, Shi J, Li Y, Deng G, Jiang Y, Li X, Zhu P, Guan Y, Bu Z, Kawaoka Y, Chen H. 2011. The PA protein directly contributes to the virulence of H5N1 avian influenza viruses in domestic ducks. *J. Virol.* 85:2180–2188. <http://dx.doi.org/10.1128/JVI.01975-10>.
- Hulse-Post DJ, Franks J, Boyd K, Salomon R, Hoffmann E, Yen HL, Webby RJ, Walker D, Nguyen TD, Webster RG. 2007. Molecular changes in the polymerase genes (PA and PB1) associated with high pathogenicity of H5N1 influenza virus in mallard ducks. *J. Virol.* 81:8515–8524. <http://dx.doi.org/10.1128/JVI.00435-07>.
- Mehle A, Dugan VG, Taubenberger JK, Doudna JA. 2012. Reassortment and mutation of the avian influenza virus polymerase PA subunit overcome species barriers. *J. Virol.* 86:1750–1757. <http://dx.doi.org/10.1128/JVI.06203-11>.
- Subbarao EK, London W, Murphy BR. 1993. A single amino acid in the PB2 gene of influenza A virus is a determinant of host range. *J. Virol.* 67:1761–1764.
- Massin P, van der Werf S, Naffakh N. 2001. Residue 627 of PB2 is a determinant of cold sensitivity in RNA replication of avian influenza viruses. *J. Virol.* 75:5398–5404. <http://dx.doi.org/10.1128/JVI.75.11.5398-5404.2001>.
- Hatta M, Gao P, Halfmann P, Kawaoka Y. 2001. Molecular basis for high virulence of Hong Kong H5N1 influenza A viruses. *Science* 293:1840–1842. <http://dx.doi.org/10.1126/science.1062882>.
- Hatta M, Hatta Y, Kim JH, Watanabe S, Shinya K, Nguyen T, Lien PS, Le QM, Kawaoka Y. 2007. Growth of H5N1 influenza A viruses in the upper respiratory tracts of mice. *PLoS Pathog.* 3:1374–1379. <http://dx.doi.org/10.1371/journal.ppat.0030133>.
- Xu C, Hu WB, Xu K, He YX, Wang TY, Chen Z, Li TX, Liu JH, Buchy P, Sun B. 2012. Amino acids 473V and 598P of PB1 from an avian-origin influenza A virus contribute to polymerase activity, especially in mammalian cells. *J. Gen. Virol.* 93:531–540. <http://dx.doi.org/10.1099/vir.0.036434-0>.
- Chu C, Fan S, Li C, Macken C, Kim JH, Hatta M, Neumann G, Kawaoka Y. 2012. Functional analysis of conserved motifs in influenza

- virus PB1 protein. *PLoS One* 7:e36113. <http://dx.doi.org/10.1371/journal.pone.0036113>.
15. Uchida Y, Watanabe C, Takemae N, Hayashi T, Oka T, Ito T, Saito T. 2012. Identification of host genes linked with the survivability of chickens infected with recombinant viruses possessing H5N1 surface antigens from a highly pathogenic avian influenza virus. *J. Virol.* 86:2686–2695. <http://dx.doi.org/10.1128/JVI.06374-11>.
 16. Mase M, Tsukamoto K, Imada T, Imai K, Tanimura N, Nakamura K, Yamamoto Y, Hitomi T, Kira T, Nakai T, Kiso M, Horimoto T, Kawaoka Y, Yamaguchi S. 2005. Characterization of H5N1 influenza A viruses isolated during the 2003–2004 influenza outbreaks in Japan. *Virology* 332:167–176. <http://dx.doi.org/10.1016/j.virol.2004.11.016>.
 17. Mase M, Eto M, Imai K, Tsukamoto K, Yamaguchi S. 2007. Characterization of H9N2 influenza A viruses isolated from chicken products imported into Japan from China. *Epidemiol. Infect.* 135:386–391. <http://dx.doi.org/10.1017/S0950268806006728>.
 18. Himly M, Foster DN, Bottoli I, Iacovoni JS, Vogt PK. 1998. The DF-1 chicken fibroblast cell line: transformation induced by diverse oncogenes and cell death resulting from infection by avian leukosis viruses. *Virology* 248:295–304. <http://dx.doi.org/10.1006/viro.1998.9290>.
 19. Hoffmann E, Stech J, Guan Y, Webster RG, Perez DR. 2001. Universal primer set for the full-length amplification of all influenza A viruses. *Arch. Virol.* 146:2275–2289. <http://dx.doi.org/10.1007/s007050170002>.
 20. Li OT, Chan MC, Leung CS, Chan RW, Guan Y, Nicholls JM, Poon LL. 2009. Full factorial analysis of mammalian and avian influenza polymerase subunits suggests a role of an efficient polymerase for virus adaptation. *PLoS One* 4:e5658. <http://dx.doi.org/10.1371/journal.pone.0005658>.
 21. Reed LJ, Muench H. 1938. A simple method of estimating fifty percent endpoints. *Am. J. Hyg.* 27:493–497.
 22. Kaplan EL, Meier P. 1958. Nonparametric estimation from incomplete observations. *J. Am. Stat. Assoc.* 53:457–481. <http://dx.doi.org/10.1080/01621459.1958.10501452>.
 23. Obayashi E, Yoshida H, Kawai F, Shibayama N, Kawaguchi A, Nagata K, Tame JR, Park SY. 2008. The structural basis for an essential subunit interaction in influenza virus RNA polymerase. *Nature* 454:1127–1131. <http://dx.doi.org/10.1038/nature07225>.
 24. Sugiyama K, Obayashi E, Kawaguchi A, Suzuki Y, Tame JR, Nagata K, Park SY. 2009. Structural insight into the essential PB1-PB2 subunit contact of the influenza virus RNA polymerase. *EMBO J.* 28:1803–1811. <http://dx.doi.org/10.1038/emboj.2009.138>.
 25. Chen H, Deng G, Li Z, Tian G, Li Y, Jiao P, Zhang L, Liu Z, Webster RG, Yu K. 2004. The evolution of H5N1 influenza viruses in ducks in southern China. *Proc. Natl. Acad. Sci. U. S. A.* 101:10452–10457. <http://dx.doi.org/10.1073/pnas.0403212101>.
 26. Leung BW, Chen H, Brownlee GG. 2010. Correlation between polymerase activity and pathogenicity in two duck H5N1 influenza viruses suggests that the polymerase contributes to pathogenicity. *Virology* 401:96–106. <http://dx.doi.org/10.1016/j.virol.2010.01.036>.
 27. Gonzalez S, Zurcher T, Ortin J. 1996. Identification of two separate domains in the influenza virus PB1 protein involved in the interaction with the PB2 and PA subunits: a model for the viral RNA polymerase structure. *Nucleic Acids Res.* 24:4456–4463. <http://dx.doi.org/10.1093/nar/24.22.4456>.
 28. Poch O, Sauvaget I, Delarue M, Tordo N. 1989. Identification of four conserved motifs among the RNA-dependent polymerase encoding elements. *EMBO J.* 8:3867–3874.
 29. Asano Y, Ishihama A. 1997. Identification of two nucleotide-binding domains on the PB1 subunit of influenza virus RNA polymerase. *J. Biochem.* 122:627–634. <http://dx.doi.org/10.1093/oxfordjournals.jbchem.a021799>.
 30. Gonzalez S, Ortin J. 1999. Distinct regions of influenza virus PB1 polymerase subunit recognize vRNA and cRNA templates. *EMBO J.* 18:3767–3775. <http://dx.doi.org/10.1093/emboj/18.13.3767>.
 31. Jung TE, Brownlee GG. 2006. A new promoter-binding site in the PB1 subunit of the influenza A virus polymerase. *J. Gen. Virol.* 87:679–688. <http://dx.doi.org/10.1099/vir.0.81453-0>.
 32. Legault P, Li J, Mogridge J, Kay LE, Greenblatt J. 1998. NMR structure of the bacteriophage lambda N peptide/boxB RNA complex: recognition of a GNRA fold by an arginine-rich motif. *Cell* 93:289–299. [http://dx.doi.org/10.1016/S0092-8674\(00\)81579-2](http://dx.doi.org/10.1016/S0092-8674(00)81579-2).
 33. Biswas SK, Nayak DP. 1994. Mutational analysis of the conserved motifs of influenza A virus polymerase basic protein 1. *J. Virol.* 68:1819–1826.
 34. He X, Zhou J, Bartlam M, Zhang R, Ma J, Lou Z, Li X, Li J, Joachimiak A, Zeng Z, Ge R, Rao Z, Liu Y. 2008. Crystal structure of the polymerase PA_C-PB1_N complex from an avian influenza H5N1 virus. *Nature* 454:1123–1126. <http://dx.doi.org/10.1038/nature07120>.
 35. Falcon AM, Marion RM, Zurcher T, Gomez P, Portela A, Nieto A, Ortin J. 2004. Defective RNA replication and late gene expression in temperature-sensitive influenza viruses expressing deleted forms of the NS1 protein. *J. Virol.* 78:3880–3888. <http://dx.doi.org/10.1128/JVI.78.8.3880-3888.2004>.
 36. Ronni T, Matikainen S, Sareneva T, Melen K, Pirhonen J, Keskinen P, Julkunen I. 1997. Regulation of IFN- α/β , MxA, 2',5'-oligoadenylate synthetase, and HLA gene expression in influenza A-infected human lung epithelial cells. *J. Immunol.* 158:2363–2374.
 37. Nimmerjahn F, Dudziak D, Dirmeier U, Hobom G, Riedel A, Schlee M, Staudt LM, Rosenwald A, Behrends U, Bornkamm GW, Mautner J. 2004. Active NF- κ B signalling is a prerequisite for influenza virus infection. *J. Gen. Virol.* 85:2347–2356. <http://dx.doi.org/10.1099/vir.0.79958-0>.
 38. Kumar N, Xin ZT, Liang Y, Ly H, Liang Y. 2008. NF- κ B signaling differentially regulates influenza virus RNA synthesis. *J. Virol.* 82:9880–9889. <http://dx.doi.org/10.1128/JVI.00909-08>.
 39. Tellier R. 2006. Review of aerosol transmission of influenza A virus. *Emerg. Infect. Dis.* 12:1657–1662. <http://dx.doi.org/10.3201/eid1211.060426>.
 40. Lyall J, Irvine RM, Sherman A, McKinley TJ, Nunez A, Purdie A, Outtrim L, Brown IH, Rolleston-Smith G, Sang H, Tiley L. 2011. Suppression of avian influenza transmission in genetically modified chickens. *Science* 331:223–226. <http://dx.doi.org/10.1126/science.1198020>.
 41. Perez DR, Donis RO. 2001. Functional analysis of PA binding by influenza A virus PB1: effects on polymerase activity and viral infectivity. *J. Virol.* 75:8127–8136. <http://dx.doi.org/10.1128/JVI.75.17.8127-8136.2001>.
 42. Wunderlich K, Juozapaitis M, Ranadheera C, Kessler U, Martin A, Eisel J, Beutling U, Frank R, Schwemmler M. 2011. Identification of high-affinity PB1-derived peptides with enhanced affinity to the PA protein of influenza A virus polymerase. *Antimicrob. Agents Chemother.* 55:696–702. <http://dx.doi.org/10.1128/AAC.01419-10>.
 43. World Health Organization. 2004. Avian influenza A(H5N1). *Wkly. Epidemiol. Rec.* 79:65–76.

Epitope Mapping of the Hemagglutinin
Molecule of A/(H1N1)pdm09 Influenza Virus
by Using Monoclonal Antibody Escape
Mutants

Yoko Matsuzaki, Kanetsu Sugawara, Mina Nakauchi,
Yoshimasa Takahashi, Taishi Onodera, Yasuko
Tsunetsugu-Yokota, Takayuki Matsumura, Manabu Ato,
Kazuo Kobayashi, Yoshitaka Shimotai, Katsumi Mizuta,
Seiji Hongo, Masato Tashiro and Eri Nobusawa
J. Virol. 2014, 88(21):12364. DOI: 10.1128/JVI.01381-14.
Published Ahead of Print 13 August 2014.

Updated information and services can be found at:
<http://jvi.asm.org/content/88/21/12364>

These include:

REFERENCES

This article cites 30 articles, 9 of which can be accessed free at:
<http://jvi.asm.org/content/88/21/12364#ref-list-1>

CONTENT ALERTS

Receive: RSS Feeds, eTOCs, free email alerts (when new
articles cite this article), [more»](#)

Information about commercial reprint orders: <http://journals.asm.org/site/misc/reprints.xhtml>
To subscribe to to another ASM Journal go to: <http://journals.asm.org/site/subscriptions/>

Epitope Mapping of the Hemagglutinin Molecule of A/(H1N1)pdm09 Influenza Virus by Using Monoclonal Antibody Escape Mutants

Yoko Matsuzaki,^a Kanetsu Sugawara,^a Mina Nakauchi,^b Yoshimasa Takahashi,^c Taishi Onodera,^c Yasuko Tsunetsugu-Yokota,^{c*} Takayuki Matsumura,^c Manabu Ato,^c Kazuo Kobayashi,^{c*} Yoshitaka Shimotai,^a Katsumi Mizuta,^d Seiji Hongo,^a Masato Tashiro,^b Eri Nobusawa^b

Department of Infectious Diseases, Yamagata University Faculty of Medicine, Yamagata, Japan^a; Influenza Virus Research Center, National Institute of Infectious Diseases, Tokyo, Japan^b; Department of Immunology, National Institute of Infectious Diseases, Tokyo, Japan^c; Department of Microbiology, Yamagata Prefectural Institute of Public Health, Yamagata, Japan^d

ABSTRACT

We determined the antigenic structure of pandemic influenza A(H1N1)pdm09 virus hemagglutinin (HA) using 599 escape mutants that were selected using 16 anti-HA monoclonal antibodies (MAbs) against A/Narita/1/2009. The sequencing of mutant HA genes revealed 43 amino acid substitutions at 24 positions in three antigenic sites, Sa, Sb, and Ca2, which were previously mapped onto A/Puerto Rico/8/34 (A/PR/8/34) HA (A. J. Caton, G. G. Brownlee, J. W. Yewdell, and W. Gerhard, *Cell* 31:417–427, 1982), and an undesignated site, i.e., amino acid residues 141, 142, 143, 171, 172, 174, 177, and 180 in the Sa site, residues 170, 173, 202, 206, 210, 211, and 212 in the Sb site, residues 151, 154, 156, 157, 158, 159, 200, and 238 in the Ca2 site, and residue 147 in the undesignated site (numbering begins at the first methionine). Sixteen MAbs were classified into four groups based on their cross-reactivity with the panel of escape mutants in the hemagglutination inhibition test. Among them, six MAbs targeting the Sa and Sb sites recognized both residues at positions 172 and 173. MAb n2 lost reactivity when mutations were introduced at positions 147, 159 (site Ca2), 170 (site Sb), and 172 (site Sa). We designated the site consisting of these residues as site Pa. From 2009 to 2013, no antigenic drift was detected for the A(H1N1)pdm09 viruses. However, if a novel variant carrying a mutation at a position involved in the epitopes of several MAbs, such as 172, appeared, such a virus would have the advantage of becoming a drift strain.

IMPORTANCE

The first influenza pandemic of the 21st century occurred in 2009 with the emergence of a novel virus originating with swine influenza, A(H1N1)pdm09. Although HA of A(H1N1)pdm09 has a common origin (1918 H1N1) with seasonal H1N1, the antigenic divergence of HA between the seasonal H1N1 and A(H1N1)pdm09 viruses gave rise to the influenza pandemic in 2009. To take precautions against the antigenic drift of the A(H1N1)pdm09 virus in the near future, it is important to identify its precise antigenic structure. To obtain various mutants that are not neutralized by MAbs, it is important to neutralize several plaque-cloned parent viruses rather than only a single parent virus. We characterized 599 escape mutants that were obtained by neutralizing four parent viruses of A(H1N1)pdm09 in the presence of 16 MAbs. Consequently, we were able to determine the details of the antigenic structure of HA, including a novel epitope.

The first influenza pandemic of the 21st century occurred in 2009. The pandemic strain, a novel swine-derived, triple reassortant A(H1N1)pdm09 (pdm09) virus, contained hemagglutinin (HA) that genetically originated with the 1918 Spanish influenza virus (1). Although the pdm09 virus was predominant in the world in the 2009/2010 and 2010/2011 influenza seasons, the A(H3N2) virus became predominant during the 2011/2012 and 2012/2013 seasons (2, 3) (see also the “Influenza virus activity in the world” website [http://www.who.int/influenza/gisrs_laboratory/updates/summaryreport_20120706/en/] and the “FluNet Summary” website [http://www.who.int/influenza/gisrs_laboratory/updates/summaryreport/en/]). The H1N1 virus was the second virus to originate with the 1918 virus, following the Russian influenza virus in 1977 (4). In the case of the Russian influenza in early 1978, most of the isolates in South America exhibited antigenic drift away from the prototype virus, A/USSR/90/77 (5). However, from 2009 to 2013, no antigenic drift was observed for the pdm09 virus, although isolates with amino acid substitutions in their antigenic sites were detected (6, 7). In 2010, viruses with double mutations in HA (N142D/E391K) were found with increased frequency in

the Southern Hemisphere (7), and it was suggested that the double mutations N142D/E391K and N142D/N173K might be associated with a reduction in the ability of vaccine sera to recognize the pdm09 virus (7, 8). Furthermore, the N173K mutation has been shown to emerge under vaccine-induced immune pressure in a ferret model of contact transmission (9). However, such viruses had not been dominant until 2013.

Antigenic mapping of H1 subtype HA was performed on A/PR/8/34 HA (PR8 HA) using variants selected by monoclonal

Received 16 May 2014 Accepted 7 August 2014

Published ahead of print 13 August 2014

Editor: A. Garcia-Sastre

Address correspondence to Eri Nobusawa, nobusawa@nih.go.jp.

* Present address: Yasuko Tsunetsugu-Yokota, Tokyo University of Technology, Tokyo, Japan; Kazuo Kobayashi, Sakai City Institute of Public Health, Osaka, Japan.

Copyright © 2014, American Society for Microbiology. All Rights Reserved.

doi:10.1128/JVI.01381-14

antibodies (MAbs), revealing the existence of four major antigenic sites, Sa, Sb, Ca, and Cb, in HA1 (10, 11). HAs of the pdm09 and A/PR/8/34 viruses originate with the Spanish influenza virus. However, pdm09 HA is directly derived from an American "triple reassortant" possessing the HA of classical swine influenza viruses (12); therefore, the antigenic regions of pdm09 HA and PR8 HA are not necessarily identical. To take precautions against antigenic drift of the pdm09 virus in the near future, it is important to determine the precise antigenic structure of pdm09 HA. In response to the 2009 pandemic, several groups elucidated the antigenic region of pdm09 HA using HA MAbs; however, a systemic analysis of the epitopes has not previously been performed (13–16).

In this study, to precisely identify antigenic regions, we have selected escape mutants of A/Narita/1/2009, the first isolate of the pdm09 virus in Japan, using 16 anti-HA MAbs. For systemic analysis of the epitopes of each MAb, we generated several parent viruses, as we did in our previous study, by considering the mutation rate during the growth of a plaque (17, 18). Thus, by using one MAb, we obtained a maximum of nine escape mutants possessing a single mutation at different positions. Finally, we isolated 599 escape mutants and identified the components of the epitopes of the 16 MAbs at four antigenic sites by cross-reactions of the escape mutants with anti-A/Narita/1/2009 HA MAbs.

MATERIALS AND METHODS

Viruses and cells. A/Narita/1/2009, a pdm09 virus, was isolated from MDCK cells and embryonated chicken eggs, which were infected with a clinical sample. The amino acid sequences of HA genes of the MDCK isolate (accession no. ACR09395) and egg isolate (accession no. ACR09396) viruses are identical. In this study, the MDCK isolate virus was propagated in MDCK cells in Dulbecco's modified Eagle medium supplemented with 0.3% bovine serum albumin and 2 µg/ml acetyl-tryptin (Sigma). Four different clones, P1, P2, P3, and P4, were obtained from well-isolated plaques of MDCK cells infected with A/Narita/1/2009 and used as parent viruses. The amino acid sequence of each parent HA was identical to that in the database (accession number ACR09395). Subsequently, seven pdm09 viruses isolated from MDCK cells from clinical samples were used for antigenic analysis: A/Yamagata/232/2009 (accession no. AB601602), A/Yamagata/752/2009 (AB601604), A/Yamagata/143/2010 (AB601605), A/Yamagata/203/2011 (AB898075), A/Yamagata/206/2011 (AB898076), A/Yamagata/264/2012 (AB898077), and A/Yamagata/87/2013 (AB898078). To examine the cross-reactivity of MAbs with seasonal H1N1 virus HA, purified HA proteins of A/Solomon Islands/3/2006 and A/Brisbane/59/2007 (Denka Seiken Co., Ltd., Tokyo, Japan) were used.

Antibodies. BALB/c mice were subcutaneously primed with 20 µg of inactivated A/Narita/1/2009 virus twice within a 3-week interval, and splenocytes were fused with Sp2/O myeloma cells at day 3 after the boosting. After limiting serial dilutions, hybridoma cells binding to A/Narita/1/2009 HA but not to A/Brisbane/59/2007 HA (H1N1) were selected by enzyme-linked immunosorbent assay (ELISA). This study was approved by the Institutional Animal Care and Use Committee of the National Institute of Infectious Diseases, Japan, and all mice were used in accordance with their guidelines.

In this study, we characterized the epitopes of the following 16 monoclonal antibodies (MAbs): NSP18 (n2), NSP30 (n3), NSP21 (n4), NSP2 (n5), NSP19 (n6), NSP22 (n7), NSP24 (n8), NSP20 (n9), NSP6 (n10), NSP26 (n11), NSP11 (n12), NSP8 (n13), NSP29 (n15), NSP27 (n16), NSP17 (n17), and NSP10 (n18). Postinfection ferret antiserum against A/California/7/2009 was used for serological assays.

Neutralization test. The virus neutralization test was performed using 6-well microplates. Mixtures of 2-fold serial dilutions of each MAb and 100 PFU of A/Narita/1/2009 were incubated for 30 min at 37°C and used

TABLE 1 Characterization of MAbs and selection frequencies of escape mutants

MAb ^a	HI titer ^b	NT ₅₀ ^c	Selection frequency (−log ₁₀) ^d			
			P1	P2	P3	P4
n2	1,280	8,000	4.41	4.54	4.29	4.06
n3	25,600	80,000	4.15	4.64	4.57	4.11
n4	25,600	80,000	3.14	4.30	4.30	3.83
n5	12,800	40,000	3.11	4.27	4.23	4.22
n6	3,200	20,000	3.13	4.40	3.99	4.21
n7	640	2,000	3.05	4.40	4.02	3.57
n8	160	400	2.97	4.22	4.09	3.75
n9	12,800	40,000	3.28	4.13	3.79	3.70
n10	6,400	20,000	3.41	3.85	3.89	3.62
n11	1,600	10,000	3.07	3.86	3.76	3.60
n12	25,600	100,000	4.08	3.96	4.32	4.13
n13	640	4,000	3.30	3.77	3.44	3.58
n15	25,600	1,600	4.02	4.40	3.03	3.38
n16	25,600	16,000	4.19	4.69	3.74	3.27
n17	25,600	100,000	4.00	4.84	4.37	4.02
n18	12,800	80,000	4.00	4.31	4.06	4.76

^a Nomenclatures for each MAbs are described in Text.

^b An HI test was performed on A/Narita/1/2009 with 0.5% turkey erythrocytes. The HI titer was expressed as the reciprocal of the highest antibody dilution which completely inhibited hemagglutination.

^c Fifty percent neutralization titers (NT₅₀) are presented as reciprocals of the highest antibody dilution causing a >50% plaque reduction, as described in the text.

^d Tenfold serial dilutions of each parent virus (P1 to P4) were mixed with 10-fold dilutions of each MAb. Escape mutants were isolated at the indicated frequency.

to inoculate MDCK cells. After 1 h, an agar overlay medium was added, and the cells were incubated at 37°C for 3 days. Neutralization titers are presented as reciprocals of the highest antibody dilution causing a >50% reduction of plaque number in 100 PFU of A/Narita/1/2009 virus.

Selection of escape mutants. The escape mutants were selected by incubating each parent virus with MAbs against A/Narita/1/2009 HA, essentially following the procedure of a previous study (17, 19). Briefly, a 10-fold serial dilution of each parental virus (P1, P2, P3, and P4) was mixed with an equal volume of a 1:10 dilution of ascites fluid containing MAbs. After incubation for 30 min at room temperature, the virus-antibody mixture was inoculated onto the MDCK cells and an agar overlay medium was added. Ten nonneutralized plaque viruses per experiment were isolated and amplified in MDCK cells. The nucleotide sequence of each mutant HA gene was determined, and the deduced amino acid sequence was compared with that of A/Narita/1/2009 HA. The antigenic character of each isolate was examined using a hemagglutination inhibition (HI) test.

Nucleotide sequencing. The nucleotide sequences of the HA genes were directly determined from RT-PCR products using the ABI Prism 3130 sequencer (Applied Biosystems). The sequences of HA primers will be provided upon request.

Radioisotope labeling and immunoprecipitation. Monolayers of MDCK cells infected with stock virus were incubated with (+TM) or without (−TM) tunicamycin (2 µg/ml) at 37°C. At 7 h postinfection, the cells were pulsed for 30 min (−TM) or 60 min (+TM) with 4 MBq/ml [³⁵S]methionine (ARC) and then disrupted as described previously (19). Immunoprecipitates of MAb n17 were analyzed by SDS-PAGE on 15% gels containing 4 M urea and processed for analysis by fluorography.

RESULTS

Selection of escape mutants of A/Narita/1/2009. We have generated 16 MAbs with neutralizing activity against A/Narita/1/2009 HA. The HI titers and neutralization titers of the MAbs are shown in Table 1. To localize the antigenic sites on pdm09 HA, we se-

lected escape mutants of the A/Narita/1/2009 strain using these MABs. Four parent viruses (P1, P2, P3, and P4) were neutralized with each of the 16 MABs, and nonneutralized plaque viruses were then analyzed as described in Materials and Methods. Escape mutants resistant to each MAB were isolated with a frequency ranging from $10^{-2.97}$ to $10^{-4.84}$ (Table 1). Consequently, we isolated 599 escape mutants with a single amino acid substitution in the HA1 domain; 157, 147, 148, and 147 mutants were derived from P1, P2, P3, and P4, respectively. These mutants were classified into 43 groups, which had different amino acid substitutions at 24 positions. By neutralizing the parent viruses derived from more than one plaque, we were able to obtain various mutants carrying different mutations (Table 2).

Antigenic sites revealed by reactivities of MABs with escape mutants in HI tests. In Fig. 1, the 24 positions are shown on the primary sequence of A/Narita/1/2009 HA1 and compared with the corresponding positions within 1918 Spanish influenza virus HA, seasonal H1N1 virus HA, and A/PR/8/34-Mt. Sinai strain HA (PR8-Mt.Sinai HA) (10).

The reactivity of each MAB with the panel of escape mutants was examined using an HI test (Table 2). Based on their reactivities, the MABs were assembled into four complementary groups: Sa (n3 to n13), Sb (n15 and n16), Ca2 (n17 and n18), and n2.

(i) Site Sa. Single amino acid changes at positions 141, 142, 171, 172, and 180 in the Sa site affected the reactions of the mutants with MABs n3 to n8, whereas the reactivities of MABs n9 to n13 with the mutants was affected by amino acid substitutions at positions 141, 142, 171, 172, and 177 (except for n13) at site Sa. Further mutations at positions 143 and 174 in the Sa site and position 173 in the Sb site affected the reactivity with n4 to n6, n4 to n10, and n9 to n13, respectively. MABs n9 and n10 lost reactivity when mutations were present at position 173, whereas n11 to n13 reacted with N173I but not with N173D. These results indicate that (i) the Sa site of Narita HA is composed of the residues at positions 141, 142, 143, 171, 172, 173, 174, 177, and 180, and (ii) there are two distinct regions in the Sa site that are recognized differently by MABs n3 to n8 and MABs n9 to n13 (Tables 2 and 3).

(ii) Site Sb. Mutations at positions 170, 173, 202, 206, 210, 211, and 212 in site Sb affected reactivity with n15 and n16. Interestingly, n15 showed decreased reactivity with G172V (Sa site) but reacted with G172E. Similar to residue 173, residue 172 also belonged to epitopes in sites Sa and Sb, depending on the amino acid residue (Tables 2 and 3).

In this study, single-mutation mutants containing H143Y (Sa site) or Q210E or N211D (Sb site) did not react with MABs n4 to n6, n15, or n15/n16, respectively, as shown in the HI test. However, they reacted well with MABs n7, n11, and n10/n11, respectively, even these MABs were used for the selection of those mutants (Table 2).

(iii) Site Ca2. In this study, two epitopes of n17 and n18 were identified in the Ca2 site. The HI reactivity of n17 and n18 with each escape mutant indicated that their epitopes are composed of residues at positions 151, 154, 156, 157, 158, 159, 200, and 238; however, the reactivity of each MAB differed based on the substituted amino acid residue, which implies that the amino acid sequences are different for the paratope of each MAB (Tables 2 and 3).

(iv) Site Pa. Three escape mutants, each possessing a single mutation at position 147, 170, or 172, were selected by MAB n2. Moreover, n2 showed decreased reactivity with the other mutant, carrying a K159N change, which was selected by n17 (Table 2). The n2 epitope presumably consisted of the residues at positions 147, 159, 170, and 172, and the last three residues were located in the Ca2, Sb, and Sa sites, respectively (Table 3). A similar epitope consisting of residues K136, D144, K147, G148, K171, and G172 has been identified for the human monoclonal antibody EM4C04, which was derived from a patient infected with the pdm09 virus (13, 15). We designated this novel antigenic site Pa.

The reactivity of ferret antiserum against A/California/7/2009 with the representative escape mutants related to each antigenic site was also examined by the HI test. No mutants showed reduced reactivity with the polyclonal ferret antiserum compared to that of the parent virus (Table 2).

Characteristics of the antigenic structure of pdm09 HA. Figure 2 shows the antigenic sites of A/Narita/1/2009 HA (Fig. 2). The epitopes for the investigated MABs, except for epitope n2, were localized within the Sa, Sb, and Ca2 antigenic sites. In this study, no MABs against Ca1 or Cb were identified. The unique positions of the amino acid substitutions in the escape mutants of A/Narita/1/2009 were 147 and 200. In the three-dimensional (3-D) structure, residue 200 of site Ca2 was located next to the residues of site Sb but was far from the other components of site Ca2 in the 3-D structure (Fig. 2). Although the S200P mutation affected the reactivity with n17 and n18, this influence may be attributed to a conformational change at topologically distant sites rather than to a direct interaction between the epitope and the paratope.

Residue 147 is located near the right edge of the receptor-binding site and is near the other members of epitope n2, including residues 159, 170, and 172, in the 3-D structure. This epitope was not detected in the antigenic site of PR8-Mt. Sinai HA or several seasonal influenza viruses (H1N1) that circulated during and after 1994/1995 because of the lack of residue 147. However, because of the presence of residue 147, the Pa site may exist in the Spanish influenza virus, PR8-Cambridge strain, and seasonal H1N1 viruses that were isolated before 1994.

Acquisition of a glycosylation site is known to shield epitopes from antibody recognition. In the seasonal influenza H1N1 virus, two highly conserved glycosylation sites, at positions 142 and 177, were identified in the Sa site, but both sites were absent in pdm09 HA. In this study, a new oligosaccharide attachment site, K177N, was generated in an escape mutant that was selected by MABs n10 and n11. However, this mutant and others with K177T or K177E all reacted with the MABs targeting site Sa. Thus, to determine whether the HA mutant with K177N was modified with N-linked glycans, we compared the electrophoretic mobilities of the mutant HAs, i.e., those with K177N and K177T, in SDS-polyacrylamide gels. As shown in Fig. 3, in the absence of TM, the parental virus and both mutant HAs showed slower electrophoretic mobility than in the presence of TM, but the mobility of these HAs was similar, suggesting that an additional glycosylation did not occur at position 177 in the mutant carrying N177.

Antigenic characterization of pdm09 HA viruses from 2009 to 2013. To detect signs of antigenic drift, genetic and antigenic analyses have been extensively performed for pdm09 isolates obtained from 2009 to 2013 (6–8). Compared with the pdm09 virus,

TABLE 2 Amino acid mutations in HAs of escape mutants with their isolation efficiencies and their effects on reactivity with each MAB

Amino acid change of escape mutants	No. of escape mutants derived from parent virus					MAB(s) used for selection of escape mutants	Hemagglutination inhibition titer of MAb ^a or of ferret antiserum against pdm09 virus														Ferret antiserum against A/California/7/2009		
							MAB at site:																
							Sa							Sb			Ca2		Pa:				
P1	P2	P3	P4	Total	n3	n4	n5	n6	n7	n8	n9	n10	n11	n12	n13	n15	n16	n17	n18	n2			
None (parent virus [P3])							12,800	12,800	12,800	3,200	640	160	12,800	6,400	2,560	25,600	640	25,600	25,600	25,600	25,600	640	1,280
P141T		3		2	5	n9, n10, n11, n13	—	—/0	—	—	—	—	0	0	0	0	0	—	—	—	—	—	NT ^b
P141L		3		3	6	n3, n8, n12	0	0	0	0	0	0	0	0	0	0	—	—	—	—	—	—	NT
N142D	10	3	10	2	25	n3, n4, n6, n7, n9, n11, n12	0	0	0	0	0	0	0	0	0	—	—	—	—	—	—	—	1,280
H143Y			2		2	n7	—	0	0	0	—	—	—	—	—	—	—	—	—	—	—	—	NT
K171E	1	3	11		15	n4–n9, n11, n12	—/0	0	0	0	0	0	0	0	0	—	—	—	—	—	—	—	NT
K171N		8	8	25	41	n3–n13	—/0	0	0	0	0	0	0	0	0	—	—	—	—	—	—	—	1,280
K171T		2	1	6	9	n3, n4, n9, n10, n12, n13	—/0	0	0	0	0	0	0	0	0	—	—	—	—	—	—	—	NT
K171Q		5			5	n12, n13	—	0	0	0	0	0	0	0	0	—	—	—	—	—	—	—	NT
G172E	40	71	45	52	208	n2, n3–n13	0	0	0	0	0	0	0	0	0	—	—	—	—	—	—	—/0	1,280
G172V	3	4			7	n12	0	0	0	0	0	0	0	0	0	—	—	—	—	—	—	—	NT
S174L	51		1	1	53	n4–n11	—	0	0	0	0	0	0	—	—	—	—	—	—	—	—	—	NT
K177N		2	1	1	4	n10, n11	—	—	—	—	—	—	—/0	0	—	—	—	—	—	—	—	—	NT
K177T	1	2			3	n11–n13	—	—	—	—	—	—	0	0	—/0	0	—	—	—	—	—	—	2,560
K177E		1		2	3	n10	—	—	—	—	—	—	0	0	—/0	0	—	—	—	—	—	—	NT
K180E		1		1	2	n3, n7	0	0	0	0	0	0	—	—	—	—	—	—	—	—	—	—	1,280
K180N				1	1	n7	0	0	0	0	0	—	—	—	—	—	—	—	—	—	—	—	NT
K170E	2	3	10	3	18	n2, n6, n8, n15, n16	—	—	—	—	—	—	—	—	—	—	0	0	—	—	—/0	NT	
K170Q		1			1	n16	—	—	—	—	—	—	—	—	—	—	0	0	—	—	—	—	NT
K170T		1			1	n15	—	—	—	—	—	—	—	—	—	—	0	0	—	—	—	—	NT
N173I	2	1			3	n9, n15	—	—	—	—	—	0	0	0	0	—	—	—	—	—	—	—	640
N173D	1	6	29	5	41	n9–n11, n13, n15, n16	—	—	—	—	—	0	0	—/0	—	—	0	0	—	—	—	—	NT
S202N		2			2	n16	—	—	—	—	—	—	—	—	—	—	0	0	—	—	—	—	1,280
Q206E			11	1	12	n15, n16	—	—	—	—	—	—	—	—	—	—	0	0	—	—	—	—	NT
Q210L		1			1	n15	—	—	—	—	—	—	—	—	—	—	0	0	—	—	—	—	NT
Q210E				1	1	n11	—	—	—	—	—	—	—	—	—	—	0	—	—	—	—	—	NT
N211D	9				9	n10, n11	—	—	—	—	—	—	—	—	—	—	0	0	—	—	—	—	NT
A212E	17	5	3	18	43	n15, n16	—	—	—	—	—	—	—	—	—	—	0	0	—	—	—	—	2,560
A151V				1	1	n17	—	—	—	—	—	—	—	—	—	—	—	0	—	—	—	—	NT
A151G	2			3	5	n17, n18	—	—	—	—	—	—	—	—	—	—	—	0	0	—	—	—	640
P154S		1	2	1	4	n18	—	—	—	—	—	—	—	—	—	—	—	—/0	0	—	—	—	NT
P154T			2		2	n18	—	—	—	—	—	—	—	—	—	—	—	—	0	—	—	—	NT
A156V		1			1	n17	—	—	—	—	—	—	—	—	—	—	—	0	—	—	—	—	NT
A156T			1	4	5	n17	—	—	—	—	—	—	—	—	—	—	—	0	—	—	—	—	NT
A156D		5	4	4	13	n17, n18	—	—	—	—	—	—	—	—	—	—	—	0	0	—	—	—	NT
G157E	15	8	4	3	30	n17, n18	—	—	—	—	—	—	—	—	—	—	—	0	0	—	—	—	NT
G157R	1				1	n18	—	—	—	—	—	—	—	—	—	—	—	—	0	—	—	—	NT
A158E		2			2	n17, n18	—	—	—	—	—	—	—	—	—	—	—	0	0	—	—	—	1,280
A158V				1	1	n18	—	—	—	—	—	—	—	—	—	—	—	—	0	—	—	—	NT
K159N	2				2	n17	—	—	—	—	—	—	—	—	—	—	—	0	0	—	0	—	1,280
S200P			1	1	2	n17, n18	—	—	—	—	—	—	—	—	—	—	—	0	—/0	—	—	—	1,280
R238K				2	2	n18	—	—	—	—	—	—	—	—	—	—	—	—	—/0	—	—	—	NT
K147N		2	1		3	n2	—	—	—	—	—	—	—	—	—	—	—	—	—/0	0	—	—	NT
K147Q				4	4	n2	—	—	—	—	—	—	—	—	—	—	—	—	—/0	0	—	—	2,560
Total no. of mutants	157	147	148	147	599																		

^a An HI test was performed with 0.5% turkey erythrocytes. The HI titer was expressed as the reciprocal of the highest antibody dilution which completely inhibited hemagglutination. —, 2- to 4-fold-lower or -higher HI titer than that with the parent virus. —/0, 8-fold lower HI titer than that with the parent virus. 0, at least 16-fold lower HI titer than that with the parent virus.

^b NT, not tested.

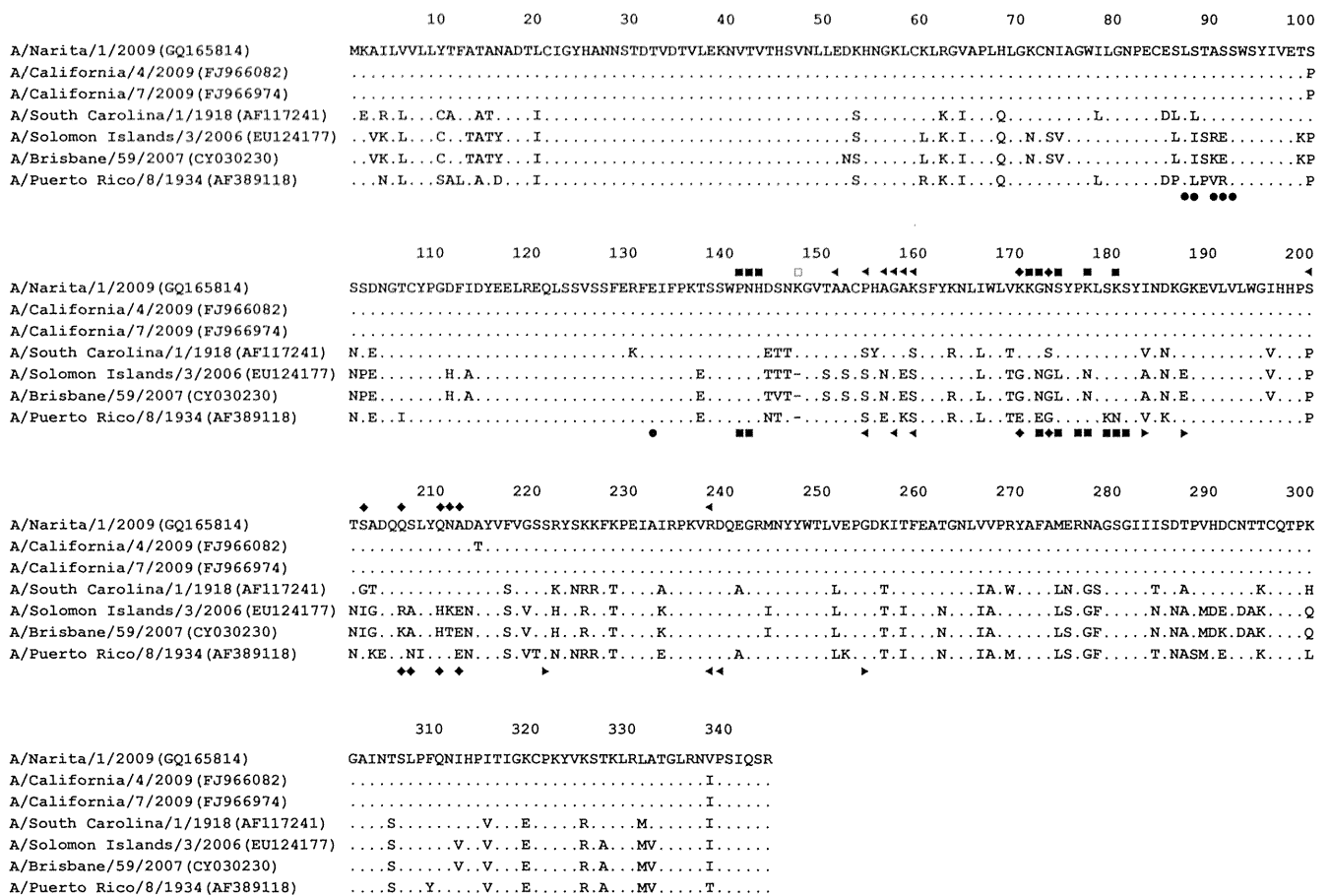


FIG 1 Comparison of the antigenic sites of HA1 among H1N1 viruses. Alignments of the amino acid sequences of the HA1 region of A/Narita/1/2009 (GenBank accession no. ACR09395), A/California/4/2009 (FJ966082), A/California/7/2009 (FJ966974), A/South Carolina/1/1918 (AF117241), A/Solomon Islands/3/2006 (EU124177), A/Brisbane/59/2007 (CY030230), and A/Puerto Rico/8/1934 (Mt. Sinai) (AF389118) are shown using H1 numbering from the first methionine in the signal peptide. Each antigenic site is shown with the corresponding symbol: ■, Sa; ◆, Sb; ▶, Ca1; ◀, Ca2; ●, Cb; □, Pa. Symbols for A/Narita/1/2009 and A/Puerto Rico/8/1934 are shown above and below the sequence, respectively.

various mutations were found at the antigenic sites of these natural isolates; however, significant antigenic differences from the A/California/7/2009 vaccine strain were not found when using ferret antiserum against A/California/7/2009 (6, 7).

To confirm that the mutations in the antigenic sites of the natural isolates affected the reactivities of the corresponding MAbs, cross-reactions of the MAbs were investigated using natural isolates obtained in Yamagata Prefecture, Japan, from 2009 to 2013. Table 4 shows the reactivities of the representative MAbs with seven representative pdm09 isolates. Among the isolates from 2009/2010, A/Yamagata/232/2009 and A/Yamagata/143/2010 reacted well with all of the investigated MAbs, whereas A/Yamagata/752/2009 failed to react with MAbs to site Sa and showed an 8-fold-lower reactivity with n2 than did A/Narita/1/2009, possibly because of the G172E mutation (sites Sa and Pa). Two other isolates from 2010-2011, A/Yamagata/203/2011 and A/Yamagata/206/2011, exhibited no or decreased reactivity with n17/n18 and n16, respectively, possibly because of the A151T/A158S/S200P (site Ca2) and S202T (site Sb) mutations. Two isolates obtained in 2012-2013, A/Yamagata/264/2012 and A/Yamagata/87/2013, showed low reactivity with n16 and n3/n7/

n16, presumably because of S202T (site Sb) and K180I/S202T (site Sa/Sb), respectively.

To determine whether any MAbs exhibit cross-reactivity with seasonal H1N1 viruses, we also examined the reactivities of 16 MAbs with A/Solomon Island/3/2006 and A/Brisbane/59/2007 HAs. No MAbs reacted well with these seasonal H1N1 virus HAs (Table 4).

During 2009 to 2013, amino acid changes at positions 202 and 220 were found in the main stream of the evolutionary pathway of these natural isolates of HA1 in Yamagata Prefecture (Fig. 4). According to the antigenic analysis of the viruses shown in Table 4, n16 lost reactivity with a S202T mutant, whereas the other mutation, S220T, which is located in the Ca1 site of PR8 HA, did not affect the reactivities of the viruses with the MAbs that were used in this study. These results show that the mutations in the antigenic site of the natural variants predictably affected reactivity with their corresponding MAbs. However, no variant lost reactivity with the ferret postinfection antiserum against A/California/7/2009, as observed for the several escape mutants in this study (Table 2). The antibodies produced in the naive ferret infected with A/California/7/2009 therefore presumably recognize more than one antigenic site of HA.